J. Earth Syst. Sci. (2024)133 156
https://doi.org/10.1007/s12040-024-02356-6

Probabilistic seismic hazard analysis of the Coimbatore region, Tamil Nadu using a logic-tree approach

Manoharan Sambath[1], Sembulichampalayam Sennimalai Chandrasekaran[2,*], Sandeep Maithani[3] and Ganapathy Pattukandan Ganapathy[2]

[1]*School of Civil Engineering, Vellore Institute of Technology, Vellore, Tamil Nadu 632 014, India.*
[2]*Centre for Disaster Mitigation and Management (CDMM), Vellore Institute of Technology, Vellore, Tamil Nadu 632 014, India.*
[3]*Urban and Regional Studies Department (URSD), Indian Institute of Remote Sensing, Dehradun, Uttarakhand 248 001, India.*
Corresponding author. e-mail: chandrasekaran.ss@vit.ac.in

MS received 14 March 2023; revised 27 February 2024; accepted 14 March 2024

The Coimbatore corporation area is comprised of very densely occupied residential and commercial buildings which are prone to future earthquakes. Probabilistic Seismic Hazard Analysis (PSHA) was carried out for the study region using the Classical Cornell approach and the logic-tree approach. A combination of 45 linear/fault sources and an areal source with a 500 km radius has been considered for the study. An updated earthquake catalogue has been compiled from various works of literature and authorized organizations. The collected earthquake catalogue of various magnitude scales has been homogenized into a uniform moment magnitude scale (M_w). Fore-shocks and after-shocks have been removed from independent events using one of the declustering algorithms. The seismicity parameters have been evaluated using the Guttenberg–Richter recurrence law. A hybrid GMPE composed of three attenuation relationships was used to obtain the ground motion parameters for the study region. The contour maps of Peak Ground Acceleration (PGA) and Peak Spectral Acceleration (PSA) for the bedrock condition have been presented in terms of 10 and 2% Probability of Exceedance (PoE) for the return period of 475 and 2475 yr, respectively. The Uniform Hazard Response Spectra (UHRS) for Coimbatore city has been compared with (IS 1893-I-(2016) Criteria for earthquake resistant design of structures. Part 1: General provisions and buildings; Bureau of Indian Standards). As a result of deaggregation, the predominant hazard has been found within a 100 km distance and no hazards have been observed from a long distance as a controlling scenario from the analysis.

Keywords. Peak ground acceleration; uniform hazard response spectrum; deaggregation analysis; probabilistic seismic hazard analysis; logic tree approach; Coimbatore corporation area.

Supplementary material pertaining to this article is available on the *Journal of Earth System Science website* (http://www.ias.ac.in/Journals/Journal_of_Earth_System_Science).

Published online: 06 August 2024

1. Introduction

Earthquakes are one of the natural hazards that have devastating effects on human life and property. Earthquakes have occurred across the globe, and the frequency of these earthquakes has been increasing annually, which causes a major impact on the economy of the nation. Notable major earthquakes across the world, such as the Iran earthquake of Richter magnitude 6.6 in 2003, caused fatalities of around 26,000 people. This is because of the northward movement of the Arabian plate against the Eurasian plate (Abolghasemi *et al.* 2006; Motamedi *et al.* 2012). The list of major earthquakes across the globe as well as Peninsular India (PI) have been illustrated in table 1.

PI has been considered a seismically stable shield region that can generate low seismicity (Bansal and Gupta 1998; Cisternas 2009). In the past decades, PI has experienced devastating earthquakes as listed in table 1 and caused many fatalities. According to the Bureau of Indian Standards IS 1893-I-(2016), these catastrophic events have changed the long-held perspective of Peninsular India's (PI) low-order seismicity and changed the seismic zonation from low to moderate seismic prone areas. Due to these catastrophic events, it is important to assess the earthquakes either by deterministic or probabilistic approach. By considering a single magnitude and distance pair, the hazard has been estimated deterministically, but the uncertainty in the source, size, and distance has been accounted for by a probabilistic approach (Cornell 1968; Kramer 1996). The Monte Carlo simulation techniques account for the uncertainty in the earthquake magnitude and distance guides to a better result (Musson 2000). Pailoplee *et al.* (2009) evaluated the seismic hazard in terms of Peak Ground Acceleration (PGA) as 2–3 g for the Thailand region using both deterministic and probabilistic approaches. The maximum spectral acceleration (S_a) at a 5 Hz frequency reaches up to 150 cm/s^2 for the Switzerland region while evaluating the hazard in a probabilistic manner (Wiemer *et al.* 2009). The Design Basis Earthquake (DBE) for Yemen has been found in the range of 0.2–0.3 g and <0.05 g for Western and Eastern Yemen, respectively, corresponding to a 10% PoE in 50 yr (Mohindra *et al.* 2012). A new fault-based source of the PSHA approach leads to a better result rather than consideration of previous instrumental data and some areal sources PSHA approach in the Malawi region (Williams *et al.* 2023). Several PSHA works were carried out for the entire India and found that the PGA values were higher in the northern region, whereas it is lower in the southern region and PI (Basu and Nigam 1977; Jaiswal and Sinha 2007; Nath and Thingbaijam 2012; Ashish *et al.* 2016; Sreejaya *et al.* 2022). The contour maps of surface level Peak Horizontal Acceleration (PHA) have been drawn for PI using a slope map derived from Digital Elevation Model

Table 1. *List of major earthquakes across the globe and Peninsular India (PI).*

Description of the earthquake	Year	Moment magnitude (M_w)	Fatalities	References
Earthquakes across the globe				
Turkey–Syria earthquake	2023	7.8	52,000	Dal Zilio and Ampuero (2023)
Afghanistan earthquake	2022	6.0	1,000	Smriti Mallapaty (2022)
Nepal earthquake	2015	7.8	8,790	Lizundia *et al.* (2017)
Tohoku earthquake (Japan)	2011	9.1	20,000	Dunbar *et al.* (2011)
Haiti earthquake	2010	7.0	3,00,000	DesRoches *et al.* (2011)
Sichuan earthquake (China)	2008	7.9	80,000	Cheng *et al.* (2009)
Yogyakarta earthquake (Indonesia)	2006	6.4	6,000	Walter *et al.* (2008)
Kashmir earthquake (Pakistan)	2005	7.6	86,000	Hussain *et al.* (2009)
Indian Ocean earthquake (Sumatra, Indonesia)	2004	9.1	2,28,000	Vigny *et al.* (2005)
Peru earthquake	1970	7.9	70,000	Chapin *et al.* (2009); Motamedi *et al.* (2012)
Earthquakes in Peninsular India				
Bhuj earthquake	2001	7.6	20,000	Hough *et al.* (2002)
Latur earthquake	1993	6.4	11,000	Gupta (1993)
Koyna earthquake	1967	6.0	200	Gupta (2002)

(DEM) data for 10 and 2% PoE (Sitharam *et al.* 2015). As an earthquake analyst, one should choose wisely both the Ground Motion Prediction Equations (GMPE's) and the suitable weights used in the logic-tree approach to account for aleatory and temporal uncertainties (Basu and Nigam 1977; Kulkarni *et al.* 1984; Sabetta *et al.* 2005; Roshan and Basu 2010; Anbazhagan *et al.* 2019). Using the stochastic seismological model, Raghu Kanth and Iyengar (2007) generated a GMPE for PI and compared the analyzed results with strong earthquakes and it is widely used in recent studies. The probabilistic and deterministic approaches led to similar hazard results for the Bangalore region (Anbazhagan *et al.* 2009). A small increment in the PGA values w.r.t. codal provisions needs much more attention for the design of structures and preparation of hazard vulnerability maps for South India (Vipin *et al.* 2009). A more accurate ground motion model is essential for Tamil Nadu to evaluate the seismic hazard for various return periods (Menon *et al.* 2010). Panza *et al.* (2011) clearly distinguished the hazard and risk and carried out Seismic Hazard Analysis (SHA) in a scientific manner which is helpful for developing countries. Most of the western and north-western parts of Chennai were exposed to moderate hazards, and the remaining areas were exposed to low hazards using the weighted-average method in the GIS overlay (Ganapathy 2011). The seismic hazard for the Kakrapar nuclear power plant in Gujarat has shown a PGA value ranging from 0.05 to 0.2 g, which is slightly less when compared to the PGA values of the seismic zonation map (Mohanty and Verma 2013). Using sub-surface rupture phenomena, Anbazhagan *et al.* (2014) estimated the rock-level PGA for the Coimbatore region corresponds to different return periods and located the most probable locations of future earthquakes. Mohanty *et al.* (2015) addressed the hazard assessment using two first-order Markov models for northeast India. Singh *et al.* (2015) carried out PSHA for Warangal city using a single seismogenic source zone and determined that the spectral values were larger for longer periods. As a result of DSHA, Elayaraja *et al.* (2015) determined that the most potential sources for the Nilgiris are Moyar and Bhavani shears. For a maximum potential magnitude of $m_{\max}$ of 6.80, the probable PGA at the bedrock level was found to be 0.156 g. A combined risk assessment of PSHA and Land-Use (LU) Hazard mapping has been evaluated for Mangalore, India (Ramkrishnan *et al.* 2019) which states that the city exposed to a PGA ranging from 0.0498 to 0.1087 g and 0.0466 to 0.0496 g for 2 and 10% PoE, respectively. The SHA has been evaluated for some parts of the Indo-Gangetic plains and obtained a PGA value of 0.062 and 0.1033 g for 475 and 2475-yr return periods, respectively (Keshri *et al.* 2020). A detailed seismicity estimation for Warangal in Peninsular India, Khan *et al.* (2020), shows a PGA value of 0.069 and 0.131 g for 475 and 2475-yr return periods, respectively. The seismic hazard has been evaluated for northeast India, and it shows that the Itanagar region has higher PGA values of 10 and 2% PoE than any other region in the vicinity of the study area (Borah and Kumar 2023).

An earthquake magnitude of 5.6 shook Indonesia in November 2022, causing a fatality of 268 people and injuring more than 100 people. This is because the focus of the earthquake is shallow, which is <10 km, and occurred in the vicinity of Jakarta, the capital of Indonesia, having densely occupied buildings that could not withstand this earthquake. In terms of magnitude scale, the city will be exposed to moderate damages, but the shallow focus of these earthquakes (<25 km) caused severe damage to the structures and led to more fatalities (Mandal *et al.* 2000; Dattatrayam and Suresh 2004; Elayaraja *et al.* 2015). It is notably important that Coimbatore city also more densely occupied and lacks earthquake-resistant structures. The city will be exposed to severe vulnerability if an earthquake happens in the future. In this present investigation, PSHA has been performed for Coimbatore city in order to develop hazard maps w.r.t. 10 and 2% PoE corresponding to 475 and 2475 yr return periods, respectively.

2. Framework of the study

This section describes the PSHA framework that has been carried out for the Coimbatore corporation area. The detailed steps are described in figure 1.

3. Study area and its tectonic setting

Coimbatore city municipal corporation area located in the western part of Tamil Nadu state, India, has been chosen as the study area for carrying out the PSHA framework. The headquarters of the Coimbatore district is the Coimbatore city with latitude 11.0168°N and longitude 76.9558°E. It is located at 411 m above Mean Sea Level

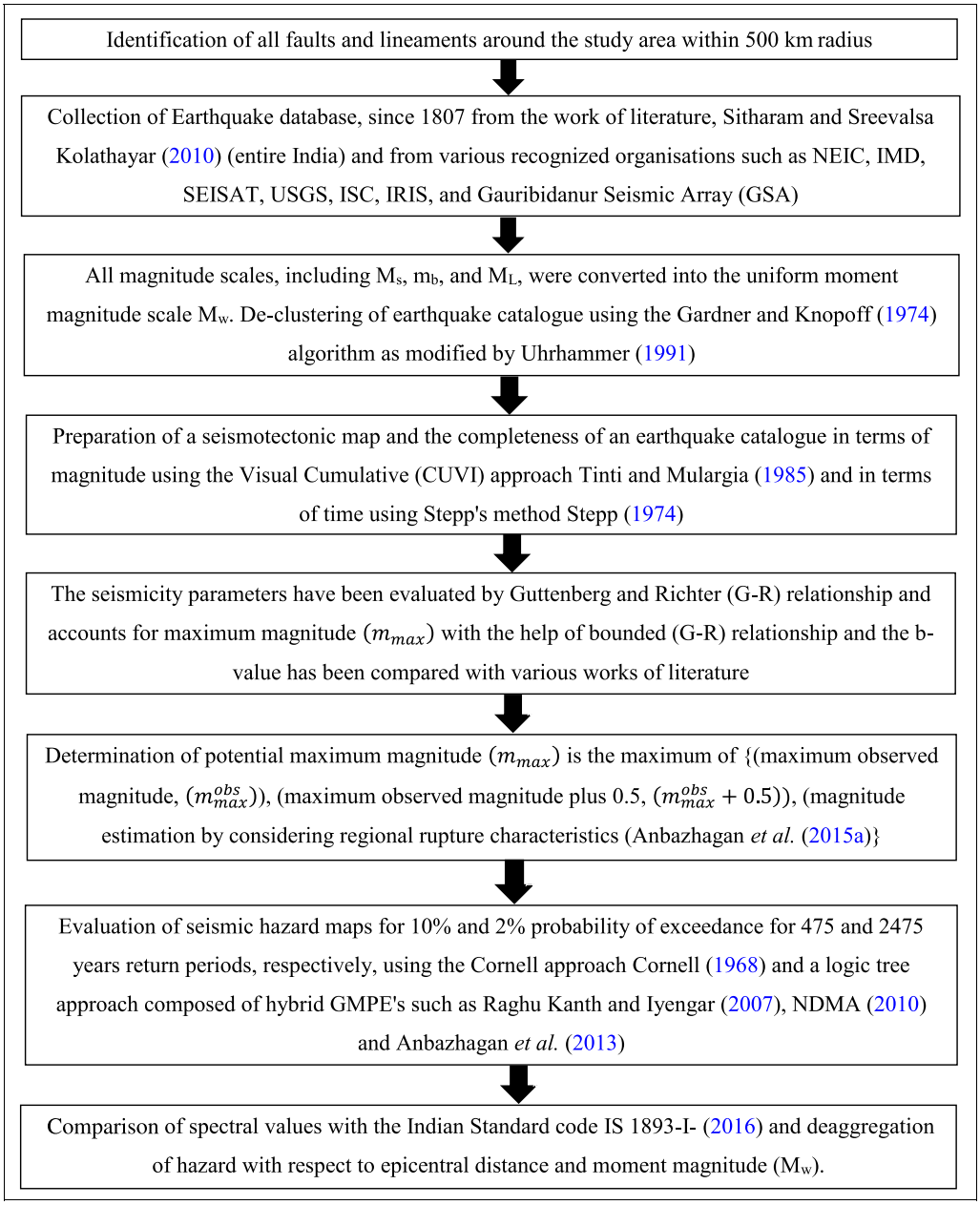

Figure 1. The framework of PSHA.

(MSL). Coimbatore is the third-largest city in the state and is known as the 'Manchester of South India'. According to the census of India 2021, the city population increased by about 15% as compared to the population in 2011. The city is famous for the manufacture of textiles which led to the textile boom in the early 1990s and has a mixture of more than 25,000 small, medium, and large size industries are present to manufacture different goods. The city is well-known for many educational institutions, and hi-tech software IT parks and is known to be an educational hub of South India. Perhaps most of the buildings within the boundary lack earthquake-resistant structures and need some attention to resist future earthquakes, if any. This study deals with the area that was exposed to more vulnerability and brings some attention to the design engineers and planners. Figure 2 depicts the study area of the present research work.

According to the Indian Standard Code IS 1893-I-(2016), Coimbatore is located in Seismic Zone III. The Coimbatore earthquake, which occurred on February 8, 1900, had a maximum intensity scale of VII in the epicentral region and a focal depth of 70 km, with a magnitude of 6.0 assigned to it (SEISAT

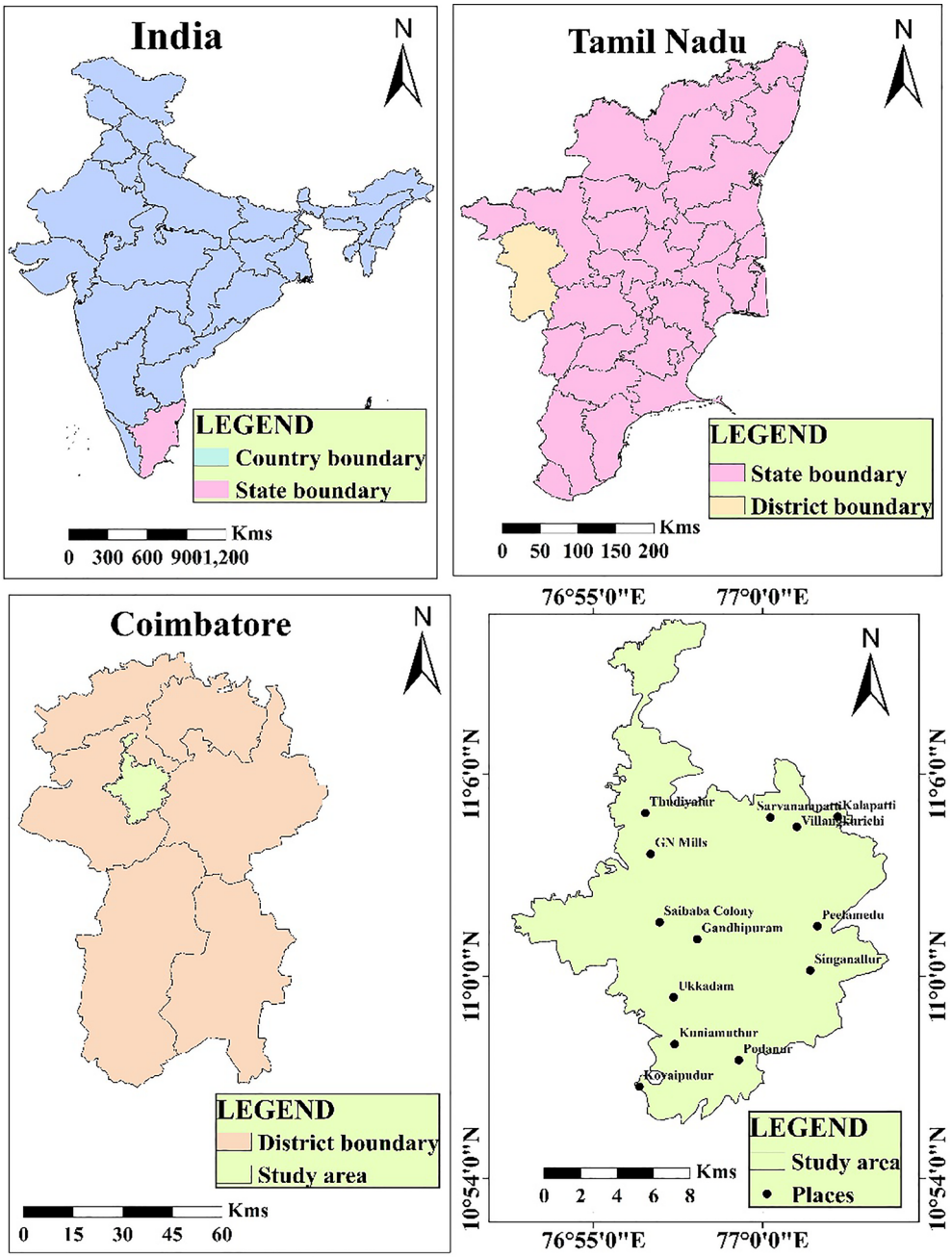

Figure 2. Study area.

2000). This event caused severe damage and destruction to buildings and houses (Basu 1964). Many tectonic faults and shear zones are present in and around the Coimbatore region with a radius of 500 km, which is the main focus of our study and evaluation of seismic hazards. There are 41 tectonic faults and four tectonic shear zones (https://bhukosh.gsi.gov.in) identified within the 500 km radius and which is shown in figure 3. In the vicinity of the study area, the Cauvery fault possesses a larger weak zone of about 348 km and has an epicentral distance of 8 km from Coimbatore city. It is considered a major source of the earthquake impact and similarly, the Periyar fault, Bhavani–Kanumudi fault, Tiruppur fault, and shear zones of Moyar and Bhavani shear zones are shown in figure 3.

4. Earthquake catalogue

The earthquake catalogue was compiled from works of literature, primarily for South India by Sitharam and Kolathayar (2018). The earthquake catalogue has also been retrieved from various recognized agencies like the International Seismological Centre (ISC) (http://www.isc.ac.uk/isc-ehb/

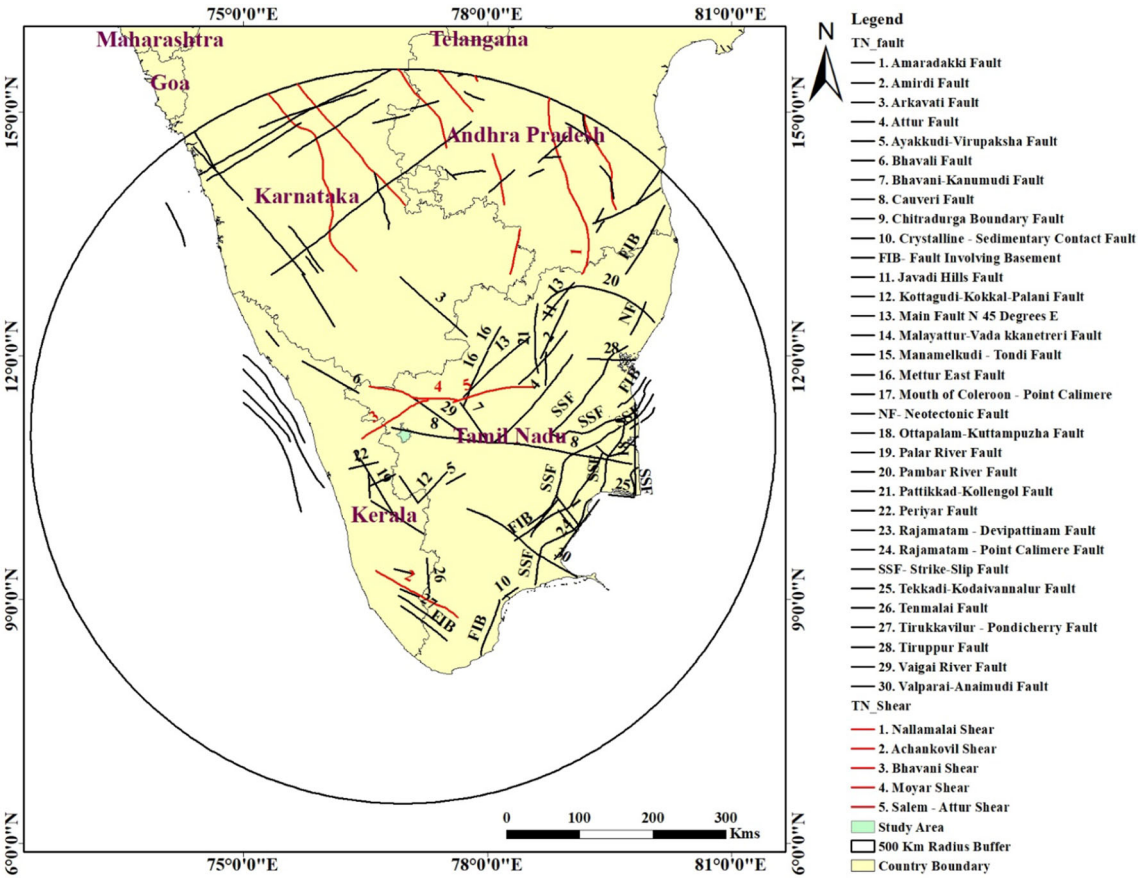

Figure 3. Tectonic faults and shear zones around the Coimbatore region.

search/catalogue/), India Meteorological Department (IMD) (https://mausam.imd.gov.in/), National Earthquake Information Centre (NEIC) (https://seismo.gov.in/MIS/riseq/Earthquake/archive), SEISAT (https://data.gov.in/keywords/seisat), USGS (https://earthquake.usgs.gov/earthquakes/search/) and Gauribidanur Seismic Array (GSA). The earthquake catalogue has been prepared for a 500 km radius in and around Coimbatore city with latitude and longitude of 11.01680°N and 76.95580°E, respectively. A compiled earthquake catalogue of 457 events since 1806 AD is shown in figure 4(a), with various magnitude scales like m_b and M_S has been homogenized into a uniform magnitude scale of moment magnitude M_w using the following equation (1) to equation (3) given by Scordilis (2006) and NDMA (2010).

$$M_w = 0.67M_S + 2.07, \text{ for } (3.0 \le M_S \le 6.1) \quad (1)$$

$$M_w = 0.99M_S + 0.08, \text{ for } (6.2 \le M_S \le 8.2) \quad (2)$$

$$M_w = 0.85m_b + 1.03, \text{ for } (3.5 \le m_b \le 6.2). \quad (3)$$

4.1 *Declustering of earthquake catalogue*

The earthquake events that were collected from NEIC, ISC, IRIS, etc., have a repetition of events, and they have been neglected with the help of comparing time, distance from the epicenter, and magnitude. For the design of structures, the earthquake events of $M_w < 3.0$ have been considered minor events and neglected from the earthquake catalogue events (Ornthammarath *et al.* 2008). The earthquake catalogue comprising of foreshocks, aftershocks, and mainshocks events has been identified and declustered using the algorithm of Gardner and Knopoff (1974) and Uhrhammer (1991). The declustering process was done in Z-MAP Software (version 7.1) Wiemer (2001), which is in date, time, and magnitude format. Finally, the declustered earthquake catalogue of about 381 events has been digitalized in ArcGIS and shown in figure 4(b). After declustering, the faults map and magnitude catalogue map were combined to create a seismotectonic map of the research area within a 500 km radius. This map

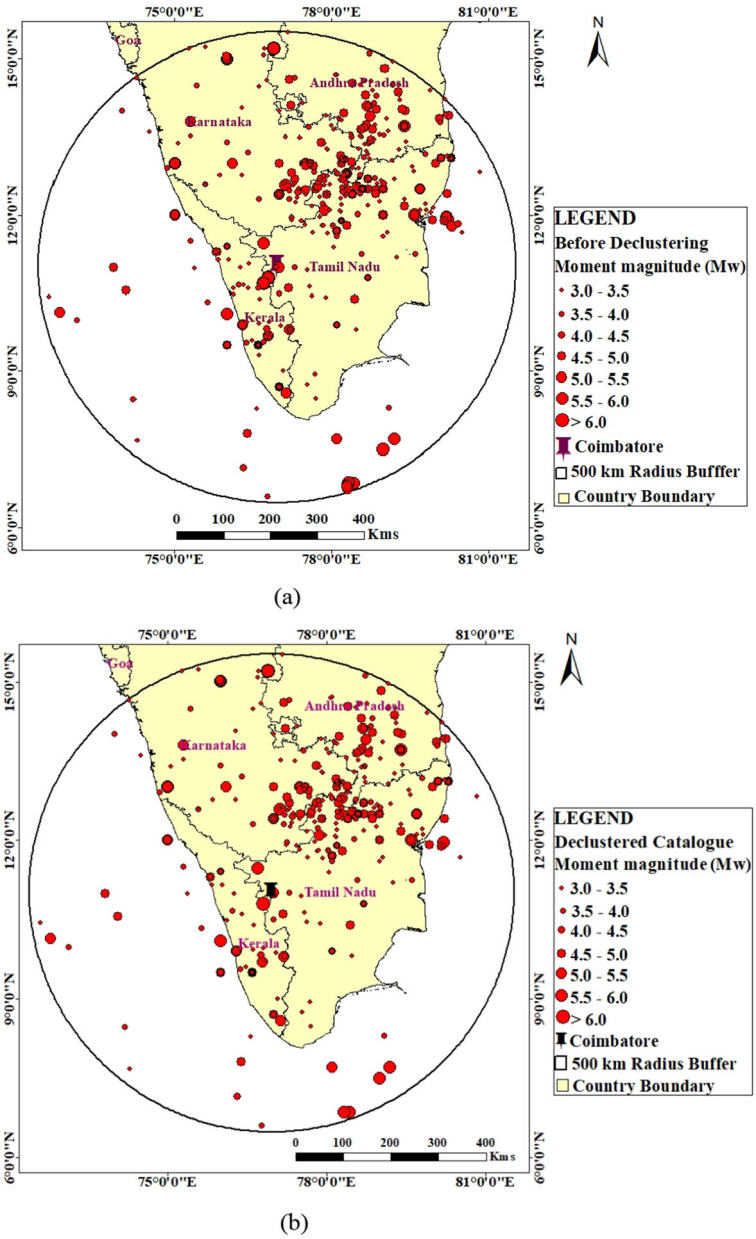

Figure 4. Moment magnitude catalogue (**a**) before declustering and (**b**) after declustering.

was digitalized in ArcGIS and is depicted in figure 5.

4.2 *Completeness analysis of earthquake catalogue*

4.2.1 *Visual Cumulative (CUVI) method*

The smaller earthquake events occur frequently whereas the larger events occur rarely within the collected timespan. The Visual Cumulative method (CUVI), which was introduced by Tinti and Mulargia (1985), and Stepp's method (Stepp 1974) have both been used for the completeness analysis. In the CUVI method, the collected earthquake events after declustering have been grouped incrementally with a common interval of 0.5 as 3.0–3.49, 3.5–3.99, 4.0–4.49, 4.5–4.99, 5.0–5.49, 5.5–5.99 and ≥6.0, respectively. A graph plot between the cumulative earthquake events was taken on the horizontal axis, while the time period was taken on the vertical axis. The corresponding year after which cumulative earthquake events should possess a linear relationship with the time has to be considered complete and has been used for further analysis. Therefore, smaller earthquake events should be complete for a finite period, whereas larger events like ≥5.0 should be

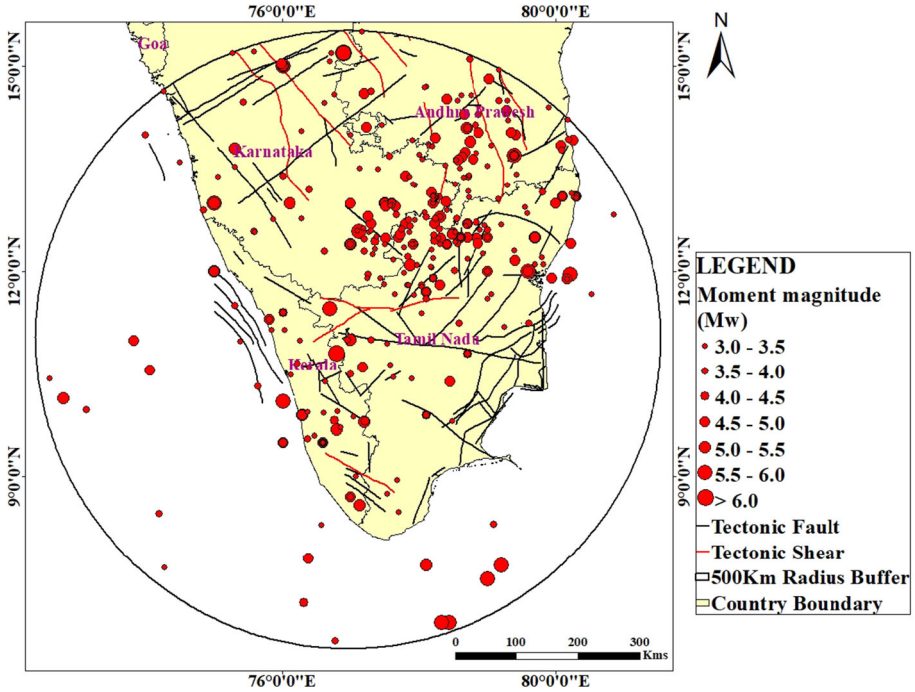

Figure 5. Seismotectonic map of the Coimbatore region.

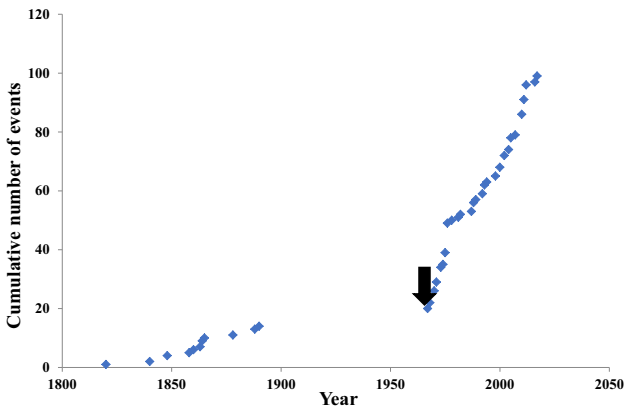

Figure 6. Completeness analysis using CUVI method for $M_w = 3.5$ to 3.99.

considered complete for the entire period. The period of completeness by the CUVI method for the magnitude range 3.5–3.99 has been shown in figure 6 and for the remaining magnitude is shown in Supplementary figure S1.

4.2.2 *Stepp's method*

In Stepp's method (Stepp 1974), the number of events that occurred within the magnitude range has been taken into consideration for a magnitude bin size of 0.5, a subsequent time interval of 10 yr, and an annual rate of exceedance for the corresponding time-space has been calculated. A common time interval of 10 yr has been chosen as bin size from the latest year to the earliest year, such as 2008–2017, 1998–2007, 1988–1997, 1978–1987, and up to 1798–1807. Finally, a plot between the time and the standard deviation is shown in figure 7. The earthquake events follow Poisson's distribution for estimating the variance (Khan and Kalyan Kumar 2018). When the slope of the linear line changes, the period is considered to be complete, which is commonly said to be over the last n years. Table 2 depicts the period of completeness analyzed by using CUVI and Stepp's method for different magnitude ranges from 3.0 to 6.0.

5. Evaluation of seismicity parameters

The most important phase in the evaluation of seismic hazards is the determination of seismicity parameters. It can be found with the help of the linear recurrence relationship given by Gutenberg and Richter (1956), which has been shown in equation (4), which assumes that the earthquake events were exponentially distributed.

$$\log\lambda_m = a - bm, \tag{4}$$

where a represents the average annual number of earthquakes with a magnitude, $m \geq 0$, b represents

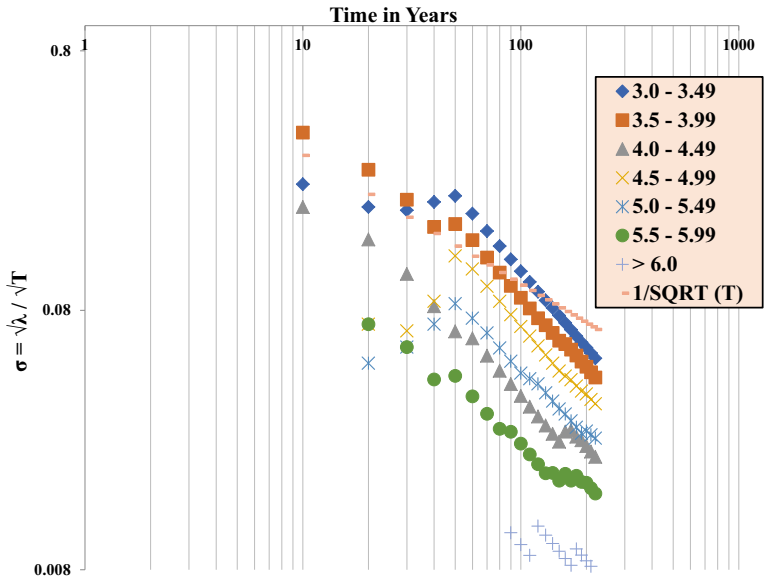

Figure 7. Analysis of completeness using Stepp's method.

Table 2. *Period of completeness by Visual Cumulative (CUVI) and Stepp's method.*

Magnitude range	CUVI method	Period of completeness	Stepp's method	Period of completeness
3.0–3.49	1967–2017	50	1967–2017	50
3.5–3.99	1967–2017	50	1967–2017	50
4.0–4.49	1958–2017	59	1957–2017	60
4.5–5.0	1958–2017	59	1957–2017	60
5.0–5.49	1952–2017	65	1952–2017	65
5.5–5.99	1937–2017	80	1937–2017	80
≥6.0	1842–2017	175	1842–2017	175

the relative likelihood of large and small earthquakes, and λ_m represents the total number of earthquake events with a magnitude of m (Gutenberg and Richter 1956). The b parameter was more sensitive when evaluating the seismic hazard. Figure 8 illustrates the Guttenberg–Richter recurrence relationship for the areal source. Figure 8 shows that the values for a and b are 3.76 and 0.86, respectively. This indicates that relatively low seismicity is expected in the study region during the hazard (Tsapanos 1990). The b values have been compared with the various works of literature, which have been shown in table 3, and imply that the Coimbatore region was prone to smaller magnitude earthquakes rather than larger events (Bilim 2019).

The exponential distribution of the G–R relationship has been modified and accounts for maximum magnitude and hence, bounded Guttenberg–Richter relationship law (Mcguire and Arabasz 1985) enters into equation (4) as given by equation (5).

$$\lambda_m = \mu \frac{\exp(-\beta(m - m_{\min})) - \exp(-\beta(m_{\max} - m_{\min}))}{1 - \exp(-\beta(m_{\max} - m_{\min}))} \tag{5}$$

where $\mu = \exp(\alpha - \beta^* m_{\min})$, $\alpha = 2.303 \times a$; $\beta = 2.303 \times b$, $m_{\min}$ = minimum magnitude and $m_{\max}$ = maximum magnitude, respectively.

5.1 *Evaluation of potential maximum magnitude* (m_u)

The determination of the maximum magnitude ($m_{\max}$) is more important in evaluating the safe design of structures. The evaluation of maximum magnitude ($m_{\max}$) will be of immense use to seismologists, disaster management agencies, etc. In this method, the maximum magnitude observed in

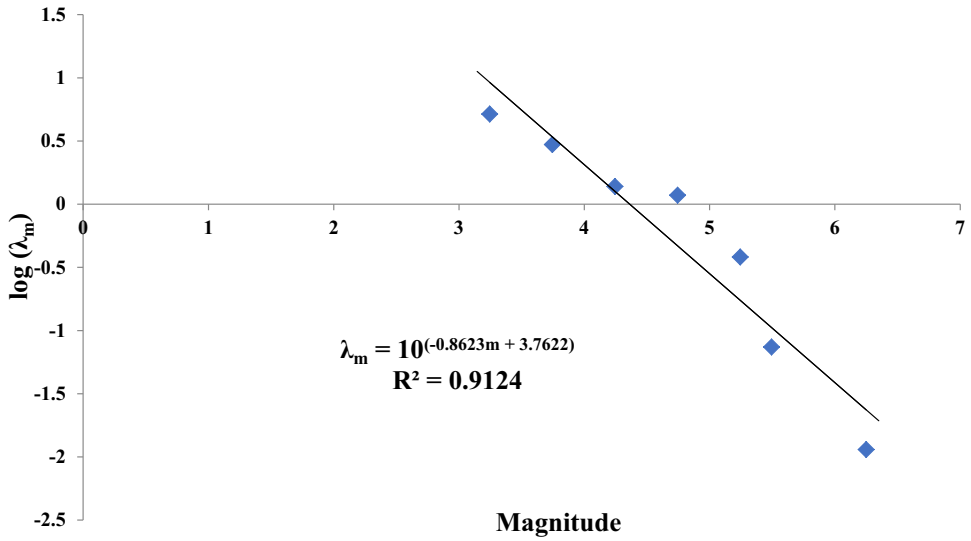

Figure 8. Guttenberg–Richter recurrence relationship for the areal source.

Table 3. *Comparison of b-values with various works of literature.*

Sl. no.	Authors	*b*-value	Study region	Data analyzed in years
1	Raghu Kanth and Iyengar (2006)	0.86	Mumbai	408
2	Jaiswal and Sinha (2006)	0.84–1.0	Peninsular India	160
3	Anbazhagan *et al.* (2009)	0.62–0.98	Bangalore	153
4	Sitharam *et al.* (2012)	0.92	Karnataka	400
5	Shukla and Choudhury (2012)	0.51	Gujarat	188
6	Patil *et al.* (2018)	0.83	Vijayapura	259
7	Anbazhagan *et al.* (2019)	0.97	Patna	400
8	Khan *et al.* (2020)	0.72–0.97	Warangal	216
9	Present study	0.86	Coimbatore	175

the earthquake catalogue in the vicinity of the study area has been given in equation (6) as

$$m_u = \max \begin{cases} \text{Maximum observed magnitude, } \left(m_{\text{obs}}^{\max}\right) \\ \text{Maximum observed magnitude} + 0.5, \left(m_{\text{obs}}^{\max} + 0.5\right) \\ \text{Considering rupture characteristics by Anbazhagan } et\ al. (2015). \end{cases} \quad (6)$$

The evaluation of the potential maximum magnitude (m_u), determined by Anbazhagan *et al.* (2015) which, accounts for the regional rupture characteristics of the region. This method has less standard error when compared to other methods of maximum magnitude estimation. The tectonic faults in the study region have been divided into three different bins based on each fault length (km) to estimate the worst-case percentage fault rupture (PFR) which is shown in table 4. The ratio of PFR for the worst-case scenario (WS) to the maximum PFR of each bin is greater than unity for all the three cases. The ratio of PFR to the total fault length (TFL) is unique for the particular region, which represents the regional rupture characteristics of the particular region and the corresponding study area (Huded and Dash 2022). Table 5 represents the worst-case RLD for each fault and estimated m_u varies from 6.1 to 6.7. Figure 9 shows the plot between the PFR and the TFL for the study area.

Table 4. *Regional rupture characteristics of three different bins of various fault lengths.*

Length of faults in each bin (km)	PFR (as %TFL)			PFR (as %TFL) for worst-case scenario (WS)	PFR for WS/maximum PFR
	Maximum	Average	Minimum		
0–80 km	41.33	22.39	3.44	45	1.09
80–200 km	12.06	6.93	1.79	16	1.33
>200 km	3.82	2.76	1.69	6	1.57

5.2 *Fault level recurrence*

The recurrence relationship for the seismic areal source zone has been estimated using equation (4), and it is also important to study the fault-level recurrence of all 45 faults, which is used in this study (NDMA 2010). The Geological Survey of India (GSI) has compiled linear seismic sources from the web (https://bhukosh.gsi.gov.in) in the vicinity of the study region for the entire India. It is critical to distinguish between the activity rates of several seismic source zones. The crucial step is to plot a frequency–magnitude relationship for each unique source. It is extremely difficult to predict the seismicity characteristics for particular faults using equation (4) due to a lack of sufficient earthquake data (Jaiswal and Sinha 2006). An alternative method is to determine the *b*-value by measuring the slip rate of the fault (Thaker *et al.* 2012). No slip values have been available for those considered areas. It is difficult to evaluate the recurrence relationship for individual faults due to a lack of information on fault characteristics. Furthermore, earthquakes in PI are associated with poor surface expressions of faults, making reliable estimation of slip rates difficult (Rajendran and Rajendran 2003; Raghu Kanth and Iyengar 2006). Hence, an approach suggested by Raghu Kanth and Iyengar (2006) based on a heuristic basis invoking the principle of conservation of seismic activity is adopted in this study. Vipin *et al.* (2009) and Anbazhagan *et al.* (2009) used this approach for the corresponding regions of PI and Bangalore. According to the theory of conservation of seismic activity by Raghu Kanth and Iyengar (2006), the seismicity rate of individual faults must be equal to the overall seismicity of that region (i.e., $N_{(m_0)} = \sum N_{i(m_0)}$), where N_i stands for the annual frequency of earthquakes ($M_w \geq 3.0$) on the ith source in the region ($i = 1, 2, 3, \ldots$).

Based on the distribution of seismic events associated with each specific fault, a weighting factor η_i is used, which is shown in equation (7).

$$\eta_i = \frac{\text{Number of earthquake events associated with that source}}{\text{Total number of earthquake events in the region}} \tag{7}$$

and where μ_i is a different weighting factor shown in equation (8), which represents the proportion of each fault's length (L_i) to the overall length of all the faults ($\sum L_i$).

$$\mu_i = \frac{L_i}{\sum L_i}. \tag{8}$$

The estimated recurrence relation for the corresponding ith fault is then estimated as the average of two weighting factors, which is depicted in equation (9).

$$N_{i(m_0)} = 0.5(\eta_i + \mu_i)N_{(m_0)}. \tag{9}$$

For the seismic hazard estimation, m_0 has been fixed as 3.0 for all the seismic sources, because less than a magnitude of 3.0, cannot cause significant damage to the structures. The notation L_i represents the length of the respective ith fault, whereas the $\sum L_i$ represents the summation of the length of all faults present in that particular zone. The value of $N_{i(m_0)}$ represents the *a*-value of a particular ith fault, and the *b*-value has been fixed as constant, which is equal to the regional *b*-values estimated from the recurrence relationship (equation 4). Detailed weightage factors for the corresponding 45 linear/fault sources are shown in table 6. The fault level recurrence for the linear and

Table 5. *Estimated m_u and worst-case RLD for each fault of the study area.*

Sl. no.	Fault name	Fault length (km)	Worst-case RLD (km)	Estimated m_u
1	Kumadavati–Narihalla fault	143.204	5.85	6.4
2	Chitradurga Boundary shear	219.385	3.82	6.7
3	Shear zone	287.963	0.29	6.7
4	Bhadra lineament	118.753	4.69	6.4
5	Vedavati lineament	337.196	1.89	6.7
6	Nallamalai shear	251.3813	1.69	6.7
7	Cuddapah Eastern Margin shear	139.772	1.54	6.4
8	Shear zone	62.578	3.44	6
9	Arkavati fault	120.48	1.79	6.4
10	Amirdi fault	96.71	1.94	6.4
11	Attur fault	160.19	1.02	6.4
12	Ayakkudi–Virupaksha fault	29.13	1.10	6
13	Bhavali fault	23.81	69.38	6
14	Bhavani shear	104.41	12.06	6.4
15	Bhavani–Kanumudi fault	60.98	31.03	6
16	Cauvery fault	326.88	1.70	6.7
17	Chitradurga Boundary fault	80.9	2.32	6
18	Crystalline-sedimentary fault	26.17	18.59	6
19	Javadi Hills fault	87.5	3.70	6.4
20	Kottagudi–Kokkal–Palani fault	58.36	0.55	6
21	Main fault (N 45°E) (ID_762)	120.67	2.34	6.4
22	Main fault N 45° E (ID_599)	66	4.28	6
23	Malayattur–Vadakanetreri	35.63	1.36	6
24	Mettur East fault	36.47	5.15	6
25	Moyar shear	120.12	10.48	6.4
26	Ottapalam–Kuttampuzha fault	98.53	1.11	6.4
27	Palar River fault	168.87	1.92	6.4
28	Pambar River fault	94.85	1.98	6.4
29	Pattikad–Kollengol fault	39.97	41.33	6
30	Periyar fault	83.92	2.94	6.4
31	Sakleshpur–Bettadpur fault	83.16	1.00	6.4
32	Tirukkavilur–Pondicherry fault	64.83	12.92	6
33	Tiruppur fault	84.62	1.46	6.4
34	Vaigai River fault	176.4	1.07	6.4
35	Valparai–Anaimudi fault	44.76	3.67	6
36	Yagachi fault	27.39	6.86	6
37	Karkambadi–Swarnamukhi fault	102.45	3.16	6.4
38	Tirumala fault	23.37	13.85	6
39	Gulcheru fault	21.3	6.72	6
40	Papaghani fault	52.56	1.58	6
41	Badvel fault	52.39	1.82	6
42	Wajrakarur fault	37.33	22.44	6
43	Gani–Kalva fault	9.1	15.74	6
44	Kumadavati–Narihalla fault	143.2	8.79	6.4
45	Cuddapah Eastern margin shear	139.77	0.60	6.4

areal seismic sources using the bounded Guttenberg–Richter relationship is depicted in figure 10(a and b). From figure 10, it is inferred that the annual probability of exceedance will be in the range of 0.008 to 0.009 for the areal sources as well as linear (fault) sources.

6. Ground motions prediction equation (GMPE)

The GMPE depends on various factors like source-to-site distance, types of fault, magnitude, propagation path, source characteristics, etc. (Dujardin

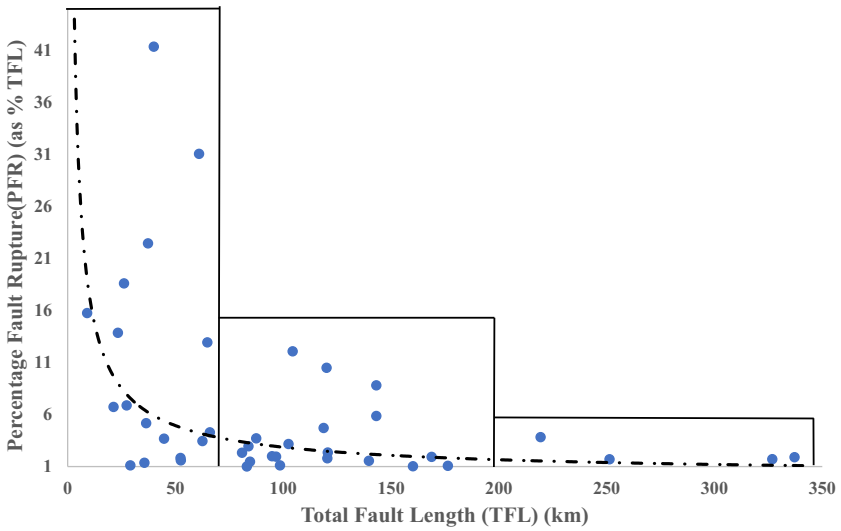

Figure 9. Plot between the PFR and the TFL for the study area.

et al. 2016). The GMPE, which has been chosen for the appropriate location, relates to the moment magnitude (M_w), epicentral distances, and fault type to the estimated values of PGA and spectral acceleration (S_a) (Douglas 2003). The first and most important step is to select the appropriate GMPE for the relevant study region because the chosen GMPE has a significant influence on the outcomes of the seismic hazard analysis. There is no ground motion predictive equation/attenuation models developed for the Coimbatore region (Anbazhagan *et al.* 2014). Anbazhagan *et al.* (2014) evaluated the best suitable GMPE equations for the Coimbatore region by efficacy test (log-likelihood (LLH)) analysis and identified NDMA (2010) as one of the best-suited GMPE equation for the Coimbatore region. Anbazhagan *et al.* (2009, 2014) and Menon *et al.* (2010) have carried out PSHA and evaluated the ground motion parameters for the region of Bangalore, Coimbatore, and entire Southern India, respectively, using the GMPE available for PI. The description of GMPEs is depicted in table 7 and the corresponding equations are shown in table 8. These GMPEs have been used by Vipin *et al.* (2009) and Menon *et al.* (2010) for the hazard estimation of the entire South India. In this study, the seismic hazard analysis was conducted using three GMPEs, namely, Raghu Kanth and Iyengar (2007), NDMA (2010), and Anbazhagan *et al.* (2013). Raghu Kanth and Iyengar (2007) and NDMA (2010) GMPEs have addressed the attenuation characteristics of Southern Peninsular India, and so the study area, which is located in that specified region, has adopted these equations. Anbazhagan *et al.* (2013) GMPE has been applied to any region-specific but more suitable to the Himalayan region and, therefore, adopted a lower weightage of 0.2 in the logic-tree approach. The NDMA (2010) GMPE is applicable for India and accounts for uncertainty by considering 32 areal sources in which the coefficients for the PI have been adopted for the study area with more weightage than the other two GMPEs. To compute the seismic hazard analysis, a hybrid GMPE (Sulastri *et al.* 2021) composed of three attenuation equations like Raghu Kanth and Iyengar (2007), NDMA (2010), and Anbazhagan *et al.* (2013) having a weightage of 0.3, 0.5, and 0.2, respectively, has been used. Instead of a single GMPE, the mean or median curve of a hybrid GMPE shows a better representation of the hazard (Sulastri *et al.* 2021).

6.1 *Logic tree approach*

The uncertainties involved in PSHA computations were broadly classified as aleatory uncertainty and epistemic uncertainty. The epistemic uncertainty arises due to various parameters like insufficient knowledge about the earthquake events, whereas the aleatory uncertainty arises due to randomness in earthquake occurrence, size of the earthquake, and the magnitude of earthquake events (Ordaz and Arroyo 2016). To minimize the epistemic uncertainty, additional data, and suitable weightage will be assigned to the different input models. The uncertainties involved in the recurrence models and maximum magnitude have to be

Table 6. *Weightage factors for the linear/fault sources in fault level recurrence.*

Fault name	Fault length (km)	Max. observed M_w $(m_{\max}^{\text{obs}})$	Estimated m_u	μ_i	η_i	$N_{i(m_0)}$
Kumadavati–Narihalla fault	143.204	5.7	6.4	0.0307	0.0106	0.0177
Chitradurga Boundary shear	219.385	5.7	6.7	0.0470	0.0158	0.0270
Shear zone	287.963	4	6.7	0.0617	0.0132	0.0321
Bhadra lineament	118.753	5.4	6.4	0.0255	0.0079	0.0143
Vedavati lineament	337.196	5.5	6.7	0.0723	0.0132	0.0367
Nallamalai shear	251.3813	5.2	6.7	0.0539	0.0475	0.0435
Cuddapah Eastern Margin shear	139.772	4.7	6.4	0.0300	0.0211	0.0219
Shear zone	62.578	4.7	6	0.0134	0.0528	0.0284
Arkavati fault	120.48	4.7	6.4	0.0258	0.1135	0.0597
Amirdi fault	96.71	4.6	6.4	0.0207	0.0106	0.0134
Attur fault	160.19	4.5	6.4	0.0344	0.0106	0.0193
Ayakkudi–Virupaksha fault	29.13	3.3	6	0.0062	0.0079	0.0061
Bhavali fault	23.81	6.2	6	0.0051	0.0053	0.0045
Bhavani shear	104.41	6	6.4	0.0224	0.0079	0.0130
Bhavani–Kanumudi fault	60.98	6.3	6	0.0131	0.0053	0.0079
Cauvery fault	326.88	5.4	6.7	0.0701	0.0185	0.0380
Chitradurga Boundary fault	80.9	4.6	6	0.0173	0.0106	0.0120
Crystalline-sedimentary fault	26.17	5.3	6	0.0056	0.0053	0.0047
Javadi Hills fault	87.5	5	6.4	0.0188	0.0185	0.0160
Kottagudi–Kokkal–Palani fault	58.36	3.3	6	0.0125	0.0053	0.0076
Main fault (N45°E) (ID_762)	120.67	4.9	6.4	0.0259	0.0264	0.0224
Main fault (N45°E) (ID_599)	66	4.9	6	0.0142	0.0106	0.0106
Malayattur–Vadakanetreri	35.63	3.6	6	0.0076	0.0079	0.0067
Mettur East fault	36.47	4.6	6	0.0078	0.0158	0.0101
Moyar shear	120.12	6	6.4	0.0258	0.0132	0.0167
Ottapalam–Kuttampuzha fault	98.53	4.2	6.4	0.0211	0.0185	0.0170
Palar River fault	168.87	5	6.4	0.0362	0.0290	0.0280
Pambar River fault	94.85	4.6	6.4	0.0203	0.0317	0.0223
Pattikad–Kollengol fault	39.97	6.2	6	0.0086	0.0053	0.0059
Periyar fault	83.92	4.8	6.4	0.0180	0.0554	0.0315
Sakleshpur–Bettadpur fault	83.16	4	6.4	0.0178	0.0132	0.0133
Tirukkavilur–Pondicherry fault	64.83	5.7	6	0.0139	0.0132	0.0116
Tiruppur fault	84.62	4.29	6.4	0.0181	0.0026	0.0089
Vaigai River fault	176.4	4.6	6.4	0.0378	0.0106	0.0207
Valparai–Anaimudi fault	44.76	4.5	6	0.0096	0.0053	0.0064
Yagachi fault	27.39	4.6	6	0.0059	0.0026	0.0036
Karkambadi–Swarnamukhi fault	102.45	5	6.4	0.0220	0.0079	0.0128
Tirumala fault	23.37	5	6	0.0050	0.0026	0.0033
Gulcheru fault	21.3	4.4	6	0.0046	0.0106	0.0065
Papaghani fault	52.56	4	6	0.0113	0.0132	0.0105
Badvel fault	52.39	4.1	6	0.0112	0.0132	0.0105
Wajrakarur fault	37.33	5.7	6	0.0080	0.0053	0.0057
Gani–Kalva fault	9.1	4.4	6	0.0020	0.0079	0.0042
Kumadavati–Narihalla fault	143.2	6	6.4	0.0307	0.0132	0.0188
Cuddapah Eastern Margin shear	139.77	4	6.4	0.0300	0.0264	0.0242

incorporated into the PSHA computations for better results. The epistemic uncertainty can be minimized using the logic tree approach by assigning appropriate weightage factors to the corresponding attenuation models (Kulkarni *et al.* 1984; Roshan and Basu 2010; Vipin and Sitharam 2013). Several nodes and branches constitute a logic tree. Each branch of the logic tree represents an individual recurrence model, each with a unique attenuation relation and a predetermined weightage. The sum of all probabilities at the branch end must be equal to unity. In this study, a logic tree

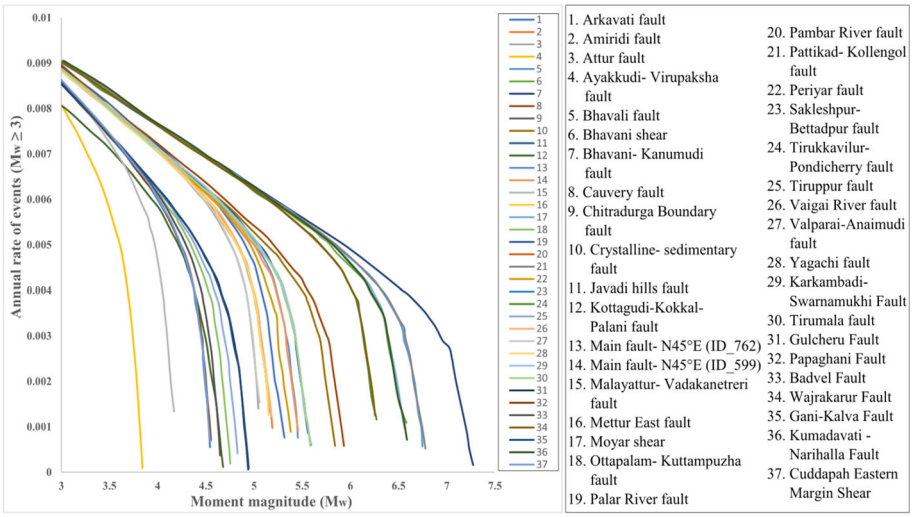

(a)

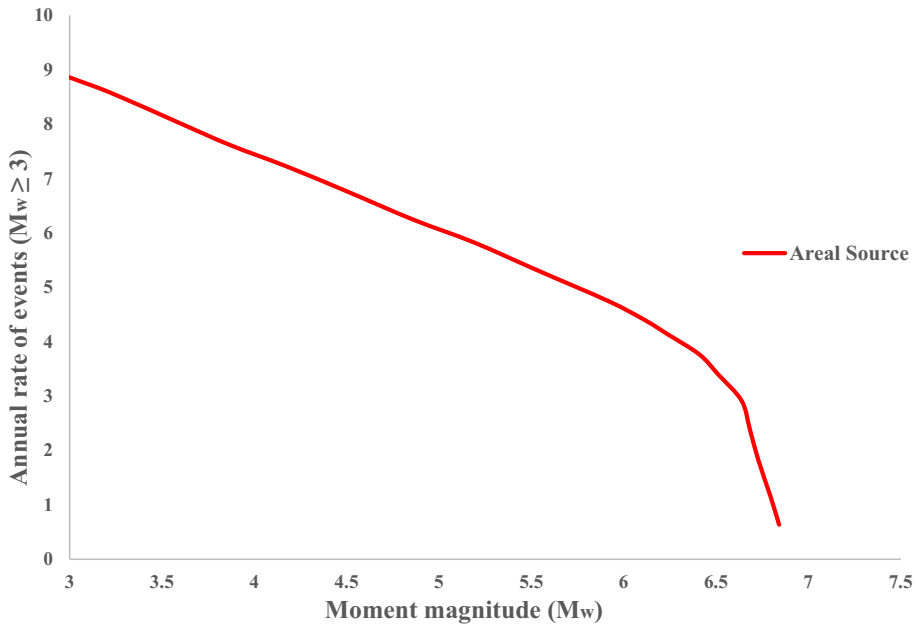

(b)

Figure 10. Magnitude–frequency relationship (**a**) linear (fault) sources and (**b**) areal sources.

Table 7. *Description of GMPE.*

GMPE	Particular region	Covered distance (km)	Period range (sec)	Moment magnitude range (M_w)
Raghu Kanth and Iyengar (2007)	Peninsular India	30–300	0.0–4.0	4.0–8.0
NDMA (2010)	Entire India	30–500	0.0–4.0	4.0–8.0
Anbazhagan *et al.* (2013)	Entire India	20–300	0.0–2.0	4.0–8.7

composed of linear/fault and areal sources having equal weightage of 0.5 with three potential maximum magnitudes such as the maximum observed magnitude $\left(m_{\max}^{\text{obs}}\right)$, maximum observed magnitude $+0.5\left(m_{\max}^{\text{obs}}+0.5\right)$, and maximum magnitude estimation by considering regional rupture characteristics (Anbazhagan *et al.* 2015) with weightage of 0.2, 0.3, and 0.5, respectively. The potential maximum magnitude estimation (m_u) by Anbazhagan *et al.* (2015) has assigned more

Table 8. *Equations of GMPE.*

GMPE-1	Raghu Kanth and Iyengar (2007) $\ln(y_{br}) = c_2 + c_2(M-6) + c_3(M-6)^2 - \ln(r) - c_4 r + \ln(\varepsilon_{br})$ where $y_{\text{br}} = (S_a/g)$ stands for the ratio of spectral acceleration at the bedrock level to acceleration due to gravity. M and r refer to moment magnitude and hypocentral distance, respectively. c_1, c_2, c_3 and c_4 are the regression coefficients. This study involves coefficients for Southern India. ε_{br} = standard deviation.
GMPE-2	National Disaster Management Authority, NDMA (2010) $\ln(\frac{S_a}{g}) = C_1 + C_2 M + C_3 M^2 + C_4 r + C_5 \ln\left(r + C_6 e^{C_7 M}\right) + C_8 f_0 \log(r) + \ln(\varepsilon)$ where $f_0 = \max(\ln(r/100), 0)$, S_a = spectral acceleration, M = moment magnitude, r = hypocentral distance (km), and C_1, C_2, C_3, C_4, C_5, C_6, C_7, and C_8 are the regression coefficients which can be found in NDMA (2010). In this research, coefficients corresponding to Peninsular India have been used.
GMPE-3	Anbazhagan *et al.* (2013) $\log(y) = c_1 + c_2 M - b\log\left(X + e^{c_3 M}\right) + (\sigma)$ where $y = S_a$ in g, M = moment magnitude, $X = \sqrt{(R^2 + h^2)}$, R= closest distance to the rupture in km, h = focal depth in km, σ = standard error term.

weightage because it has less standard deviation than the other two methods of maximum magnitude estimation. A hybrid GMPE (Sulastri *et al.* 2021) composed of Raghu Kanth and Iyengar (2007), NDMA (2010), and Anbazhagan *et al.* (2013) attenuation relations with weightage of 0.3, 0.5 and 0.2, respectively. The NDMA (2010) attenuation equation was developed for India which accounts for source uncertainty and so the study area has adopted more weightage when compared to the other two attenuation equations. A total of 18 branches with various weightage for the logic tree approach which was shown in figure 11 and the corresponding weights were shown in the parentheses.

7. Probabilistic seismic hazard analysis (PSHA)

The uncertainties due to hypocentral distance and moment magnitude (M_w) have to be addressed while evaluating the seismic hazards. The overall hazard curve for a particular site s has to be obtained by equation (10). It is noted that the overall hazard curve for the entire region is the total of all the hazard curves based on all the sources within that specific location obtained by equation (11) (Kramer 1996; Surve *et al.* 2021).

$$\lambda_{i,s} = N_i \sum_{m_i=3}^{m_{\max}} \sum_{r_j=r_0}^{r_{\max}} P\left(Y > y^* | m_i, r_j\right) \times [PDF_{ms}]_{m=m_i} \times [PDF_{rs}]_{r=r_j} \quad (10)$$

$$\lambda_s = \sum_{i=1}^{i} N_i \sum_{m_i=3}^{m_{\max}} \sum_{r_j=r_0}^{r_{\max}} P\left(Y > y^* | m_i, r_j\right) \times [PDF_{ms}]_{m=m_i} \times [PDF_{rs}]_{r=r_j}. \quad (11)$$

7.1 *Magnitude uncertainty $[PDF]_{ms}$*

The maximum probable magnitude ($m_{\max}$) for every fault has been estimated as given in section 5.1. There is a possibility that the different sizes of earthquake events have been generated by a single seismic source. A source can generate more earthquake events of smaller sizes rather than larger sizes of earthquake events (Kramer 1996). There is no possibility that a seismic source can generate an earthquake having a size of more than the maximum probable magnitude ($m_{\max}$) (Joshi and Sharma 2008). In general, a particular fault can generate an earthquake event having a size ranging from ($m_{\min}$) to ($m_{\max}$). For a particular fault, the variation of frequency of seismic events corresponds to the magnitude evaluated by the probability density function of magnitude uncertainty $[PDF]_{\text{ms}}$. In this research, the truncated exponential recurrence model (Kramer 1996; Iyengar and Ghosh 2004) has been used. The recurrence model is given by the following equation (12) as,

$$PDF_{\text{ms}} = \frac{\beta e^{-\beta(m-m_{\min})}}{1 - e^{-\beta(m_{\max}-m_{\min})}}, \quad (12)$$

where $\beta = 2.303 \times b$ and $m_{\min} \leq m \leq m_{\max}$.

This equation has been used to calculate the probability density function of magnitude uncertainty $[PDF]_{\text{ms}}$ for all faults in that area. Figure 12

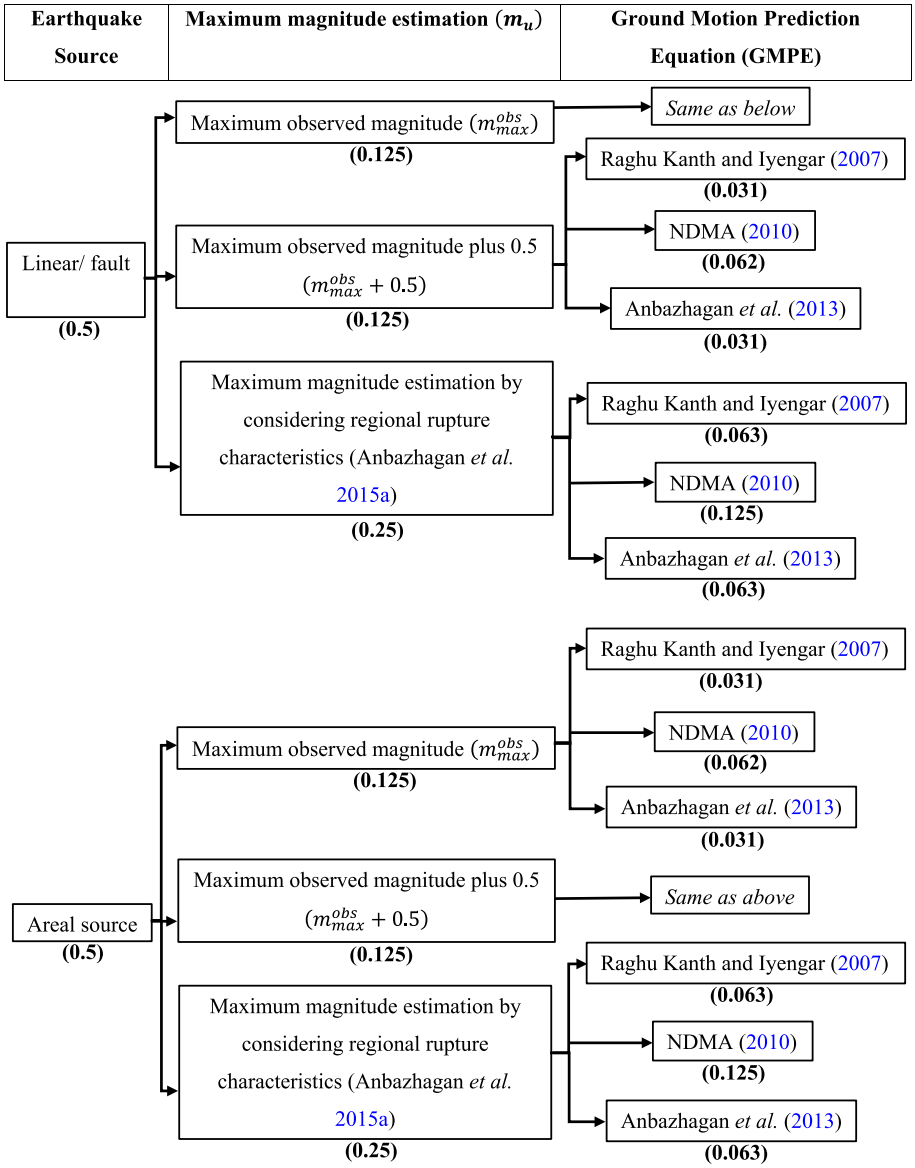

Figure 11. Logic tree approach.

depicts the $[PDF]_{\mathrm{ms}}$ of the Cauvery fault having a moment magnitude ranging from 3.0 to 6.8.

7.2 *Hypocentral distance uncertainty [PDF]$_{rs}$*

The estimate of seismic risks for the specific site of interest mainly depends on the source-to-site distance. It was considered that the seismic occurrences had an equal chance of happening everywhere inside the specific source zone. Then, hypocentral distance is said to be a random variable that corresponds to the rupture point. Thus, the resulting probability density function for the hypocentral uncertainty has been given by the following equation (13) (Charles Scawthorn 1977; Kramer 1996).

$$PDF_{\mathrm{rs}} = \frac{r}{L_i\sqrt{r^2 - r_{\mathrm{min}}^2}}, \tag{13}$$

where r_{min} is the minimum hypocentral distance from the source of interest.

For all seismic sources, this equation has been utilized to assess the probability density function of hypocentral uncertainty $[PDF]_{\mathrm{rs}}$. The Cauvery fault's $[PDF]_{\mathrm{rs}}$ are depicted in figure 13 with hypocentral distances ranging from 0 to 500 km. The estimation of hazards using the open-source software R-CRISIS 2015 version 20.3 (http://www.r-crisis.com) (Singh *et al.* 2015; Khan *et al.* 2020) has been carried out.

The Classical Cornell technique (Cornell 1968) was used to carry out the complete PSHA in this study. The study area was consistently divided into

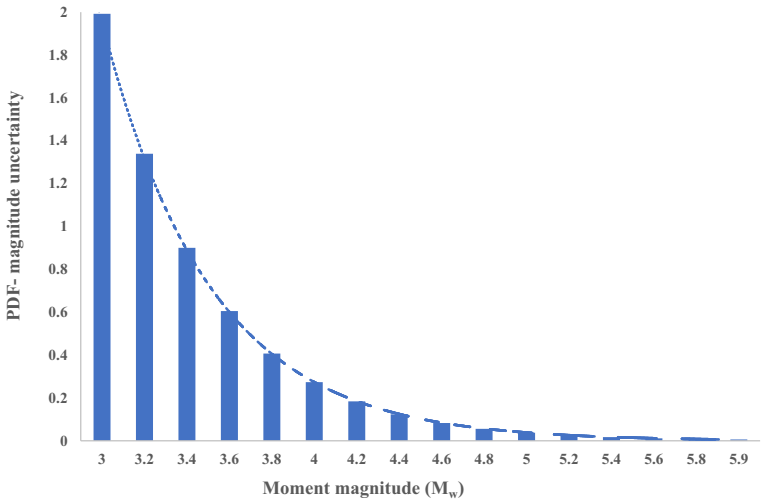

Figure 12. PDF_{ms} of magnitude uncertainty for the Cauvery fault.

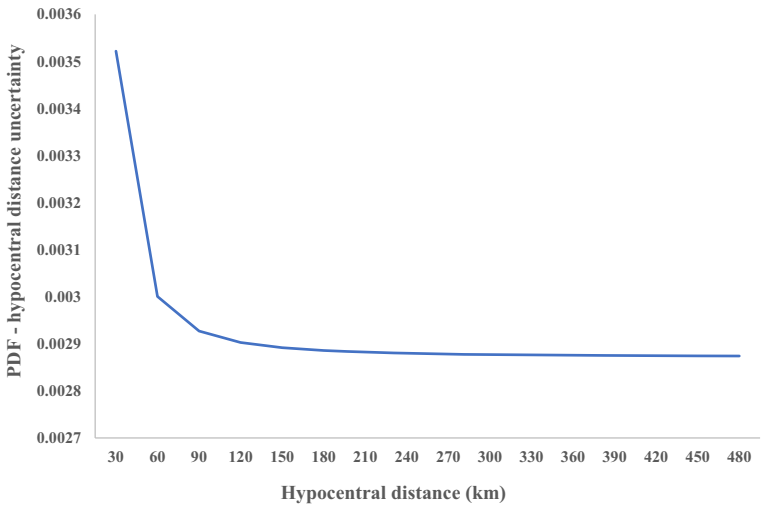

Figure 13. PDF_{rs} of hypocentral distance uncertainty for the Cauvery fault.

grids that were 0.0005° × 0.0005° in size, covering the whole of Coimbatore city within the suggested grid points. The seismic parameter has been assessed at the center of each grid point that covers the full study region for the bed-rock condition (V_s > 1500 m/s). A hybrid GMPE (Sulastri *et al.* 2021) composed of Raghu Kanth and Iyengar (2007), Anbazhagan *et al.* (2013), and NDMA (2010) equation has been used to evaluate the hazard analysis. The hazard has been evaluated using all branches of the logic tree approach with appropriate pre-defined weightage for each grid point. As a result, the hazard curves corresponding to 72, 224, 475, 975, and 2475 yr return periods, respectively, have been obtained using RCRISIS 2015 software version 20.3. The output will be in the form of the PoE of a particular intensity, which has been incorporated in ArcGIS 10.5 Desktop to prepare the hazard contour maps in terms of gravity (g) for the various return periods. The return period corresponds to a 475-yr return period known to be a Design Basis Earthquake (DBE) and similarly, a 2475-yr return period is said to be a Maximum Credible Earthquake (MCE) considered for the design of structures (Eurocode 2005).

8. Results and discussions

8.1 *Seismic hazard maps*

The entire PSHA computations for Coimbatore city have been evaluated by incorporating the uncertainties with equal weightage using the classical Cornell approach (Cornell 1968) and the logic tree approach. By using these approaches,

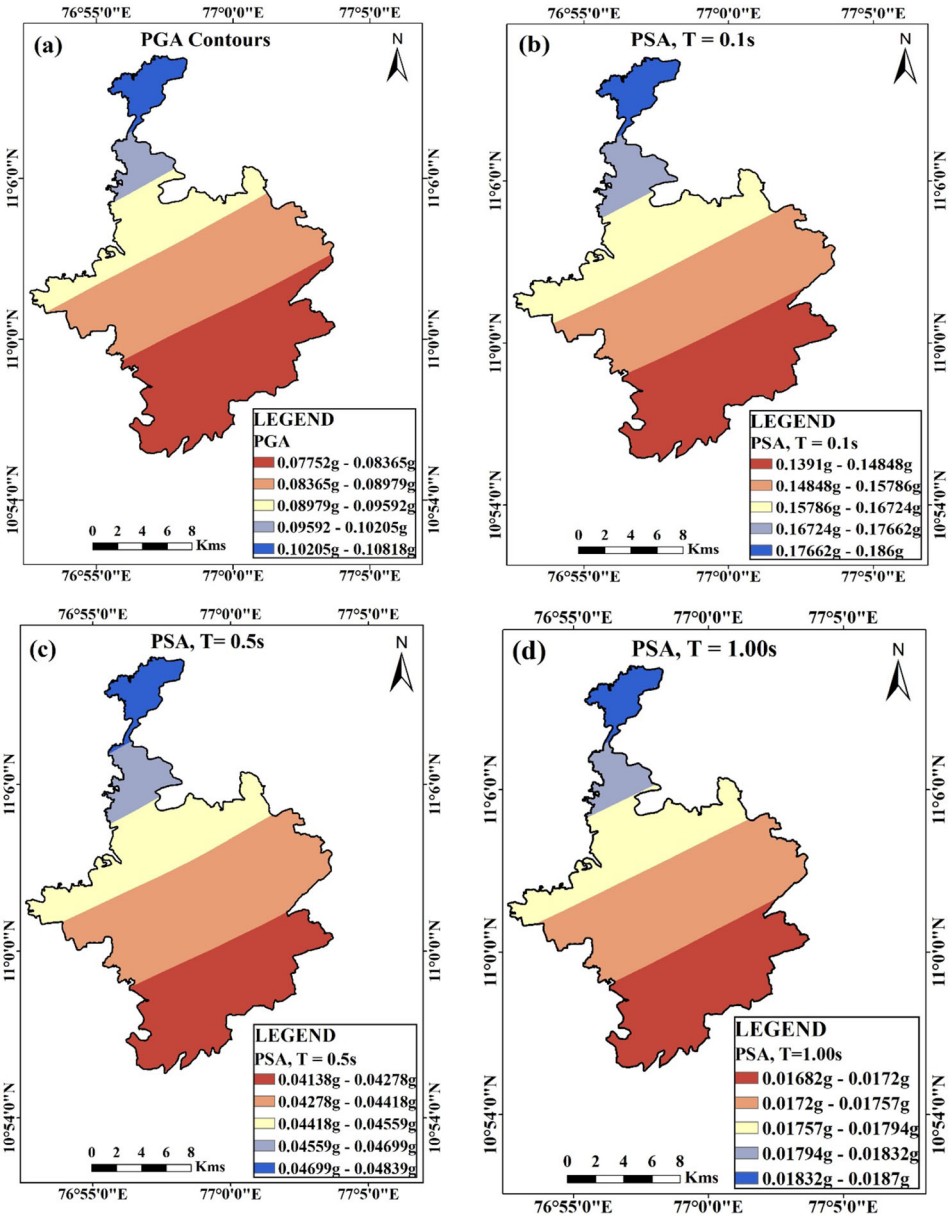

Figure 14. Spatial variation of hazard maps using Cornell approach for 10% probability of exceedance, which corresponds to 475 yr return period (**a**) PGA contours, (**b**) PSA, $T = 0.10$ sec, (**c**) PSA, $T = 0.50$ sec and (**d**) PSA, $T = 1.00$ sec.

hazard maps were created as contour maps with the help of ArcGIS 10.5 Desktop, which are illustrated in figures 14, 15, 16, 17. These hazard contour maps were expressed as the spatial variation of PGA and PSA in terms of 'g' with structural periods of $T = 0.1$, 0.5, and 1.0 sec for 10 and 2% PoE which corresponds to 475 and 2475 yr return period, respectively. From figures 14–17, it was inferred that the northern part of the study region was exposed to more bed-rock acceleration, whereas the southern part of the study region was exposed to low bed-rock acceleration. The obtained results of PGA and PSA with structural periods of $T = 0.1$, 0.5, and 1.00 sec, which have been compared with the results of Menon *et al.* (2010) hold good and match well with the results of the present study. Results are compared with Menon *et al.* (2010) depicted in table 9 for a 10 and 2% PoE, which correspond to 475 and 2475 yr of the return period, respectively. The PGA values from this research study slightly exceed the values presented by Menon *et al.* (2010) and IS 1893-I-(2016), implying that there is a need for consideration of the seismic forces to be incorporated for the careful design of structures.

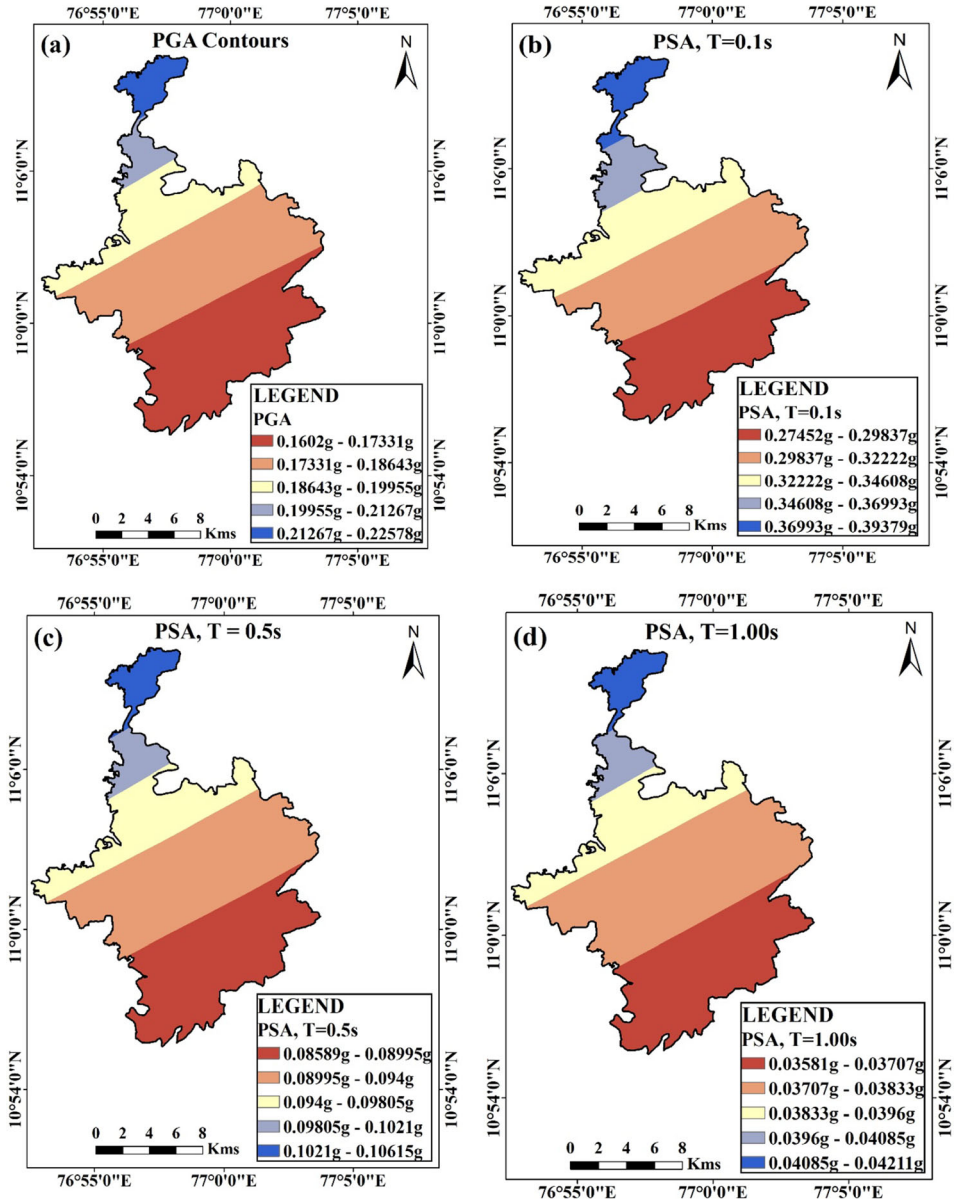

Figure 15. Spatial variation of hazard maps using Cornell approach for 2% probability of exceedance which corresponds to 2475 yr return period (**a**) PGA contours, (**b**) PSA, $T = 0.10$ sec, (**c**) PSA, $T = 0.50$ sec and (**d**) PSA, $T = 1.00$ sec.

8.2 *Uniform hazard response spectra (UHRS)*

The response spectra for the structures match the design PGA level over the full frequency range. The response spectra are used to evaluate the structures when they are subjected to dynamic loading. For the examination of structures, design response spectra have been extracted from seismic hazard curves for the same probability of exceedance across the full frequency range (Raghu Kanth and Iyengar 2006). Such response spectra were said to be Uniform Hazard Response Spectra (UHRS). For rock stratum or stiff soil, UHRS has been evaluated for a particular site within the Coimbatore city with latitude and longitude of 11.089°N and 76.941°E, respectively, for the 10 and 2% PoE, which corresponds to 475 and 2475 yr return period, respectively. The plot of UHRS with structural periods ranging from 0 to 2 sec has been shown in figure 18. The obtained spectral acceleration (S_a) values were slightly higher than the IS seismic code values IS 1893-I-(2016). The comparison of results with IS 1893-I-(2016) for the structural periods, $T = 0.1$, 0.5, and 1.00 sec have been reported in table 10. From table 10, it is inferred that at low periods the PGA values of the research area surpassed the IS 1893-I-(2016) codal values while the

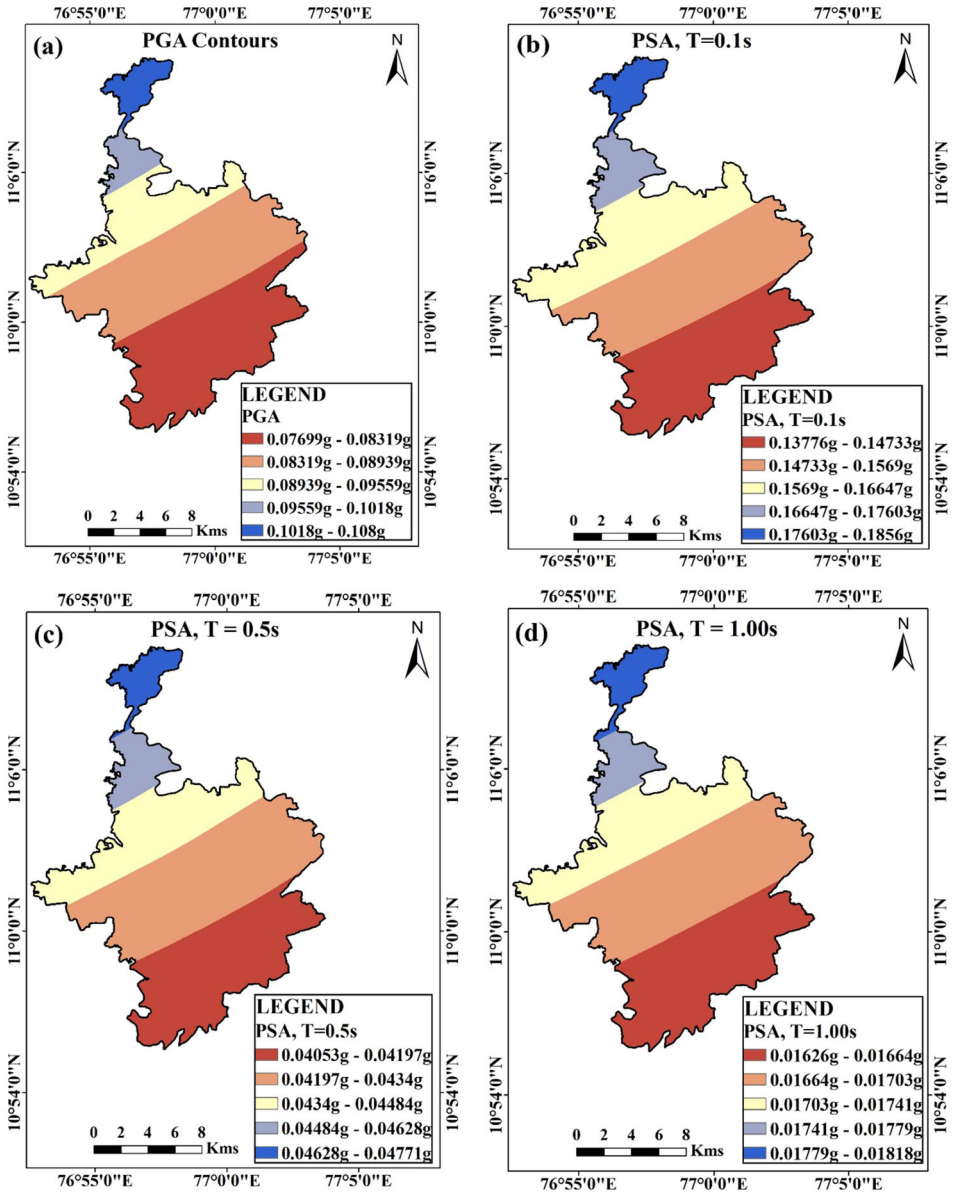

Figure 16. Spatial variation of hazard maps using logic tree approach for 10% probability of exceedance, which corresponds to 475 yr return period (**a**) PGA contours, (**b**) PSA, $T = 0.10$ sec, (**c**) PSA, $T = 0.50$ sec and (**d**) PSA, $T = 1.00$ sec.

opposite trend has been observed for longer periods.

8.3 *Deaggregation analysis*

The deaggregation analysis has been carried out to identify the predominant hazard at a particular distance for a particular moment magnitude (Peláez Montilla *et al.* 2002). It describes 'where the hazard comes from' (Kramer 1996; Peláez Montilla *et al.* 2002). Due to consideration of areal sources and the uncertainties involved in the distance and magnitude, the deaggregation analysis helps us to identify the particular moment magnitude and epicentral distance that contributes to the hazard. The deaggregation analysis has been depicted in the 3D chart, in which the x-axis represents the moment magnitude (M_w), the y-axis represents the epicentral distance (km), and the z-axis represents the exceedance probability. The deaggregation analysis was examined in the present study for a 10 and 2% PoE, corresponding to 475 and 2475 yr return periods, respectively, as depicted in figure 19. It was inferred that the predominant hazard would be at an epicentral distance of about 25 km, having a moment magnitude (M_w) of 5.24 for the 10% PoE, which corresponds to 475 yr return period. Similarly, for the 2% PoE

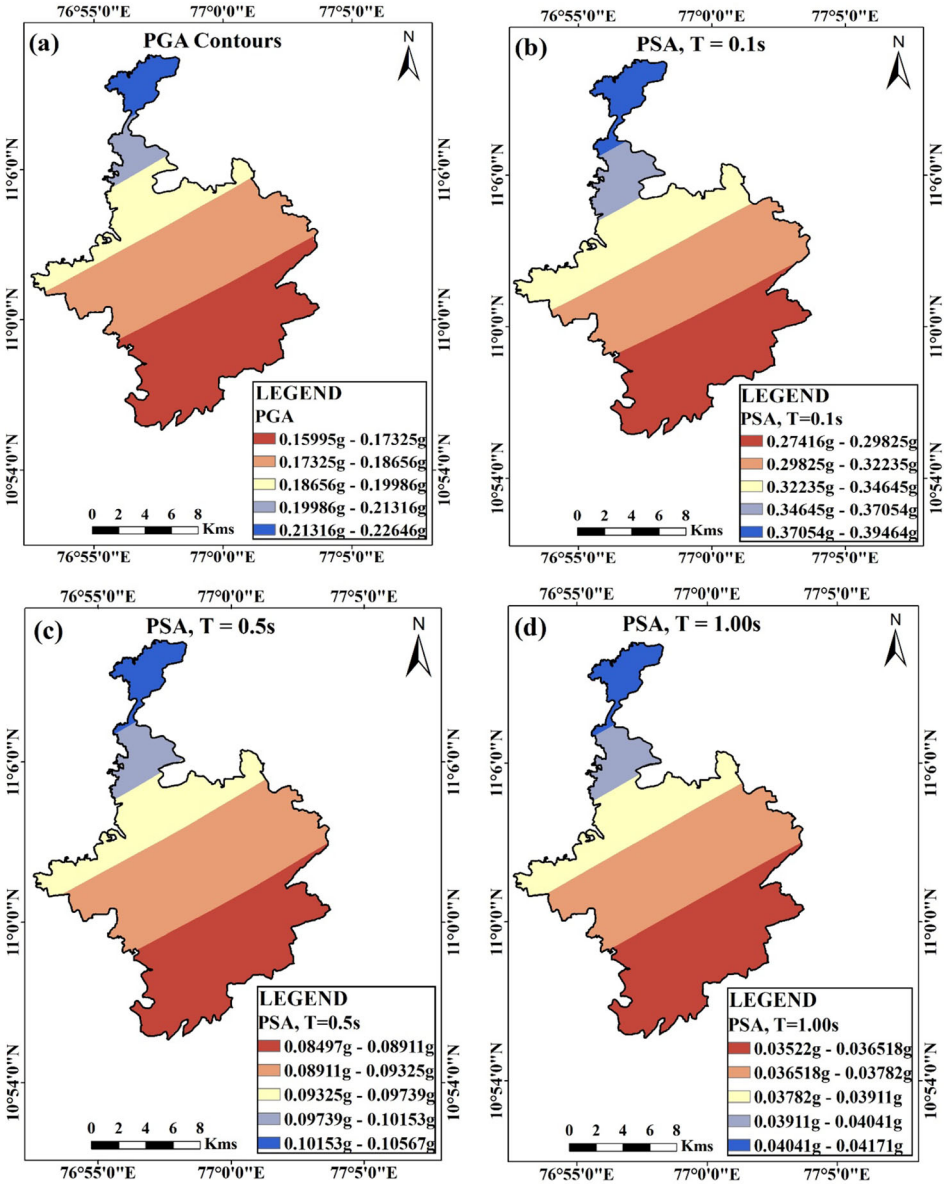

Figure 17. Spatial variation of hazard maps using logic tree approach for 2% probability of exceedance, which corresponds to 2475 yr return period (**a**) PGA contours, (**b**) PSA, $T = 0.10$ sec, (**c**) PSA, $T = 0.50$ sec and (**d**) PSA, $T = 1.00$ sec.

Table 9. *Comparison of PGA and PSA values $T = 0.1$, 0.5, and 1 sec with Menon et al. (2010) for the Coimbatore region.*

	Description Study area	Menon *et al.* (2010) Entire Tamil Nadu (Coimbatore city)	Present study Coimbatore corporation region
475 yr return period	PGA value	0.080–0.089 g	0.077–0.108 g
	PSA, $T = 0.1$ sec	0.20–0.225 g	0.1378–0.1856 g
	PSA, $T = 0.5$ sec	0.050–0.059 g	0.0405–0.0477 g
	PSA, $T = 1$ sec	0.0220–0.0239 g	0.0163–0.0182 g
2475 yr return period	PGA value	0.1575–0.175 g	0.16–0.2265 g
	PSA, $T = 0.1$ sec	0.35–0.4 g	0.2742–0.3946 g
	PSA, $T = 0.5$ sec	0.110–0.119 g	0.085–0.1057 g
	PSA, $T = 1$ sec	0.05–0.055 g	0.0352–0.0417 g

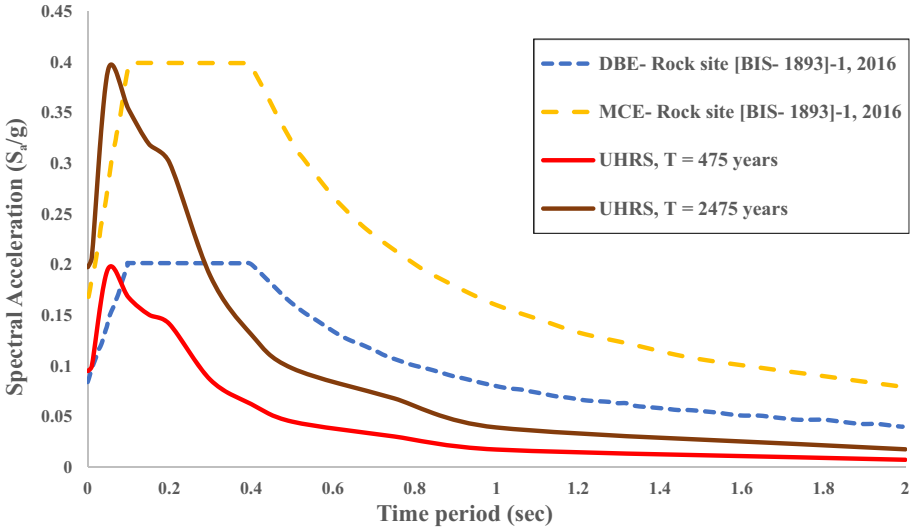

Figure 18. Uniform Hazard Response Spectra (UHRS) for 10 and 2% probability of exceedance (PoE), which corresponds to 475 and 2475 yr return period.

Table 10. *Comparison of spectral acceleration (S_a) values with IS 1893-I-(2016).*

	IS 1893-I-(2016)				Present study			
Return period (yr)	PGA $T = 0.0$ sec	PSA $T = 0.2$ sec	PSA $T = 0.5$ sec	PSA $T = 1.0$ sec	PGA $T = 0.0$ sec	PSA $T = 0.2$ sec	PSA $T = 0.5$ sec	PSA $T = 1.0$ sec
475	0.08	0.2	0.16	0.08	0.095	0.141	0.045	0.0175
2475	0.16	0.4	0.31	0.16	0.198	0.3	0.098	0.039

which corresponds to the 2475-yr return period, the predominant hazard would be at an epicentral distance of about 25 km for a moment magnitude (M_w) of 6.07. From the analysis, it has been clear that the contribution of hazard has been at a shorter distance, which is less than about 100 km in both cases, and hazards with minimum PoE exist for longer distances. These findings imply that the seismic waves impact the structures in the vicinity of a 100 km radius, and after, the seismic waves will attenuate for a larger distance.

9. Conclusions

The following conclusions have been drawn from the current study:

1. Using Gardner and Knopoff (1974) and later modified by Uhrhammer (1991) declustering algorithm, an earthquake catalogue of 381 independent events has been evaluated for completeness analysis using the Visual Cumulative (Tinti and Mulargia 1985) and Stepp's (Stepp 1974) method.
2. The seismicity parameter (b-value) has been evaluated as 0.86 for the present study using the Guttenberg and Richter recurrence relationship.
3. A hybrid GMPE (Sulastri *et al.* 2021) composed of Raghu Kanth and Iyengar (2007), Anbazhagan *et al.* (2013), and NDMA (2010) attenuation relationship has been employed to evaluate the Peak Ground Acceleration (PGA) for the bed-rock condition. To account for the epistemic uncertainty, the logic tree approach has been incorporated into this present study.
4. Using the Cornell approach (Cornell 1968), the PGA values were obtained as 0.107 and 0.2258 g, whereas, using the logic tree approach, the obtained PGA values as 0.108 and 0.226 g, which correspond to 475 and 2475 yr return periods, respectively. It was concluded from the seismic hazard maps that the southern part of the study region was subjected to low bed-rock acceleration while the northern part of the study region was exposed to more bed-rock acceleration.
5. From the Uniform Hazard Response Spectra (UHRS), the spectral acceleration (S_a/g) values

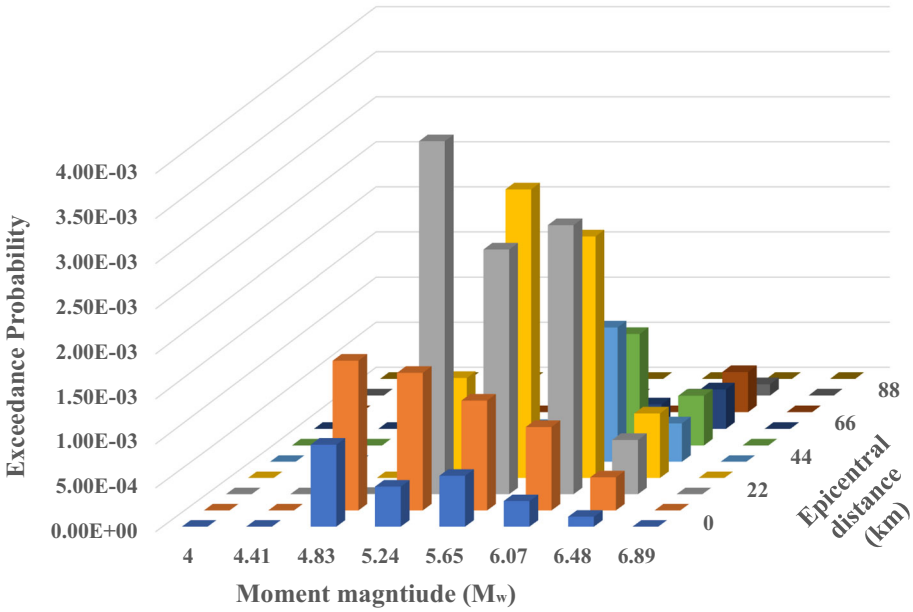

(a)

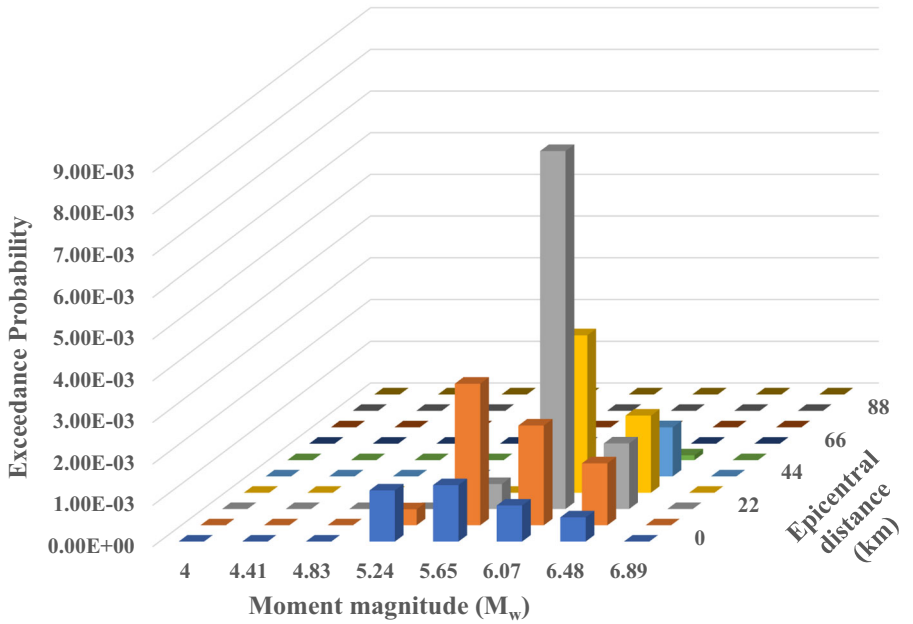

(b)

Figure 19. Deaggregation analysis (**a**) for 10% probability of exceedance corresponds to a 475-yr return period and (**b**) for 2% probability of exceedance corresponds to a 2475-yr return period.

have been evaluated, and they are slightly higher than the IS 1893-I-(2016) values. The hazard maps have been disaggregated to find out the predominant hazard. As a result, the hazard within a 100 km radius has been a controlling scenario from the analysis.

The goal of the current study is to assess the ground motion parameters and create hazard vulnerability maps, which will be useful for planners and design engineers in learning about the seismicity of the region. This study guides and promotes the design of earthquake-resistant structures in the earthquake susceptibility region. The obtained PGA corresponds to the bedrock condition and the effect of local soil conditions is not incorporated in this study. The PGA values at

the ground/foundation level may vary slightly depending upon the amplification/de-amplification effects of the local site. Based on the analysis of a few bore-log data collected, the Southern region of Coimbatore city has a low Standard Penetration Test (SPT) *N*-values which implies a slight amplification of ground motions is possible. It is recommended to update the seismicity information periodically to perform the hazard analysis.

Acknowledgements

The authors would like to thank Indian Space Research Organisation (ISRO), Government of India, for sponsoring this work through the RESPOND project titled 'Urban Seismic Risk Assessment' (Project Sanction Order ISRO/RES/4/672/19-20 dated September 11th 2019). The authors wish to thank Geological Survey of India (GSI), Bhukosh (https://bhukosh.gsi.gov.in), India Meteorological Department (IMD), National Earthquake Information Centre (NEIC), Incorporated Research Institutions for Seismology (IRIS), and International Seismological Centre (ISC) for supplying the seismicity data. The authors would like to thank the developers of the R-CRISIS team (http://www.r-crisis.com) for providing the R-CRISIS open-source application version 20.3, which has been used in the present study.

Author statement

All authors contributed to the study's conception and design. Material preparation, data collection, and analysis were performed by Manoharan Sambath. The first draft of the manuscript was written by Manoharan Sambath and all authors (Sennimalai Sembulichampalayam Chandrasekaran, Sandeep Maithani, Ganapathy Pattukandan Ganapathy) commented on previous versions of the manuscript.

References

Abolghasemi H, Radfar M H, Khatami M, Nia M S, Amid A and Briggs S M 2006 International medical response to a natural disaster: Lessons learned from the Bam earthquake experience; *Prehosp. Disaster Med.* **21** 141–147.

Anbazhagan P, Vinod J S and Sitharam T G 2009 Probabilistic seismic hazard analysis for Bangalore; *Nat. Hazards* **48** 145–166, https://doi.org/10.1007/S11069-008-9253-3.

Anbazhagan P, Kumar A and Sitharam T G 2013 Ground motion prediction equation considering combined dataset of recorded and simulated ground motions; *Soil Dyn. Earthq. Eng.* **53** 92–108, https://doi.org/10.1016/j.soildyn.2013.06.003.

Anbazhagan P, Smitha C V and Kumar A 2014 Representative seismic hazard map of Coimbatore, India; *Eng. Geol.* **171** 81–95, https://doi.org/10.1016/J.ENGGEO.2013.12.013.

Anbazhagan P, Bajaj K, Moustafa S S and Al-Arifi N S 2015 Maximum magnitude estimation considering the regional rupture characteristics; *J. Seismol.* **19(3)** 695–719, https://doi.org/10.1007/s10950-015-9488-x.

Anbazhagan P, Bajaj K, Matharu K, Moustafa S S and Al-Arifi N S 2019 Probabilistic seismic hazard analysis using the logic tree approach-Patna district (India); *Nat. Hazards Earth Syst. Sci.* **19** 2097–2115, https://doi.org/10.5194/nhess-19-2097-2019.

Ashish, Lindholm C, Parvez I A and Kühn D 2016 Probabilistic earthquake hazard assessment for Peninsular India; *J. Seismol.* **20** 629–653, https://doi.org/10.1007/s10950-015-9548-2.

Bansal B K and Gupta S 1998 A glance through the seismicity of Peninsular India GMPEs from recorded acceleration time histories for Peninsular India view project site selection of additional nuclear power plants view project: A glance through the seismicity of Peninsular India; *J. Geol. Soc. India* **52** 67–80.

Basu K L 1964 A note on the Coimbatore earthquake of 8 February 1900; *Mausam* **15** 281–286, https://doi.org/10.54302/mausam.v15i2.5544.

Basu S and Nigam N C 1977 Seismic risk analysis of Indian Peninsula; *6th World Conf. Earthq. Eng.* 782–790.

Bilim F 2019 The correlation of *b*-value in the earthquake frequency-magnitude distribution, heat flow and gravity data in the Sivas Basin, Central Eastern Turkey; Bitlis Eren University; *J. Sci. Technol.* **9** 11–15, https://doi.org/10.17678/beuscitech.467269.

Borah N and Kumar A 2023 Probabilistic seismic hazard analysis of the North-East India towards identification of contributing seismic sources; *Geomat. Nat. Haz. Risk* **14** 1–38, https://doi.org/10.1080/19475705.2022.2160662.

Chapin E, Daniels A, Elias R, Aspilcueta D and Doocy S 2009 Impact of the 2007 Ica earthquake on health facilities and health service provision in Southern Peru; *Prehosp. Disaster Med.* **24** 326–332.

Charles S 1977 A fault-rupture model for seismic risk analysis; *Bull. Seismol. Soc. Am.* **7** 541–559.

Cheng J, Liu J, Gan W and Li G 2009 Influence of coseismic deformation of the Wenchuan earthquake on the occurrence of earthquakes on active faults in Sichuan-Yunnan region; *Earthq. Sci.* **31** 477–490.

Cisternas A 2009 Montessus de ballore, a pioneer of seismology: The man and his work; *Phys. Earth Planet. Inter.* **175(1–2)** 3–7, https://doi.org/10.1016/j.pepi.2007.09.006.

Cornell C A 1968 Engineering seismic risk analysis; *Bull. Seismol. Soc. Am.* **58** 1583–1606.

Dal Zilio L and Ampuero J P 2023 Earthquake doublet in Turkey and Syria; *Commun. Earth Environ.* **4** 2–5, https://doi.org/10.1038/s43247-023-00747-z.

Dattatrayam R S and Suresh G 2004 A source study of the Bhuj, India, earthquake of 26 January 2001 (M_w 7.6); *Bull. Seismol. Soc. Am.* **94** 1195–1206.

DesRoches R, Comerio M, Eberhard M, Mooney W and Rix G J 2011 Overview of the 2010 Haiti earthquake; *Earthq. Spectra* **27** 1–21, https://doi.org/10.1193/1.3630129.

Douglas J 2003 Earthquake ground motion estimation using strong-motion records: A review of equations for the estimation of peak ground acceleration and response spectral ordinates; *Earth-Sci. Rev.* **61** 43–104, https://doi.org/10.1016/S0012-8252(02)00112-5.

Dujardin A, Courboulex F, Causse M and Traversa P 2016 Influence of source, path, and site effects on the magnitude dependence of ground-motion decay with distance; *Seismol. Res. Lett.* **87** 138–148, https://doi.org/10.1785/0220150185.

Dunbar P, McCullough H, Mungov G, Varner J and Stroker K 2011 2011 Tohoku earthquake and tsunami data available from the National Oceanic and Atmospheric Administration/National Geophysical Data Center; *Geomat. Nat. Hazards Risk* **2** 305–323, https://doi.org/10.1080/19475705.2011.632443.

Elayaraja S, Chandrasekaran S S and Ganapathy G P 2015 Evaluation of seismic hazard and potential of earthquake-induced landslides of the Nilgiris, India; *Nat. Hazards* **78** 1997–2015, https://doi.org/10.1007/S11069-015-1816-5.

Eurocode I 2005 Irish Standard Eurocode 8: Design of structures for earthquake resistance – Part 1.

Ganapathy G P 2011 First level seismic microzonation map of Chennai city – A GIS approach; *Nat. Hazards Earth Syst. Sci.* **11** 549–559, https://doi.org/10.5194/NHESS-11-549-2011.

Gardner J K and Knopoff L 1974 Is the sequence of earthquakes in Southern California, with aftershocks removed, Poissonian?; *Bull. Seismol. Soc. Am.* **64** 1363–1367, https://doi.org/10.1785/BSSA0640051363.

Gupta H K 2002 A review of recent studies of triggered earthquakes by artificial water reservoirs with special emphasis on earthquakes in Koyna, India; *Earth-Sci. Rev.* **58** 279–310, https://doi.org/10.1016/S0012-8252(02)00063-6.

Gupta H K 1993 The deadly Latur earthquake; *Science* **262(5140)** 1666–1667, https://doi.org/10.1126/science.8259511.

Gutenberg B and Richter C F 1956 Earthquake magnitude, intensity, energy, and acceleration: (Second paper); *Bull. Seismol. Soc. Am.* **46(2)** 105–145, https://doi.org/10.1785/BSSA0460020105.

Motamedi M H, Sagafinia M, Ebrahimi A, Shams E and Motamedi M K 2012 Major earthquakes of the past decade (2000–2010): A comparative review of various aspects of management; *Trauma Mon.* **17(1)** 219–229, https://doi.org/10.5812/traumamon.4519.

Hough S E, Martin S, Bilham R and Atkinson G M 2002 The 26 January 2001 M 7.6 Bhuj, India, earthquake: Observed and predicted ground motions; *Bull. Seismol. Soc. Am.* **92** 2061–2079, https://doi.org/10.1785/0120010260.

Huded P M and Dash S R 2022 Probabilistic seismic hazard assessment at bedrock level using a logic tree approach: A case study for Odisha, an Eastern State of India; *Pure Appl. Geophys.* **179** 527–549, https://doi.org/10.1007/s00024-021-02929-2.

Hussain A, Yeats R S and Lisa Mona 2009 Geological setting of the 8 October 2005 Kashmir earthquake; *J. Seismol.* **13** 315–325, https://doi.org/10.1007/s10950-008-9101-7.

IS 1893 (Part 1) 2016 Criteria for earthquake resistant design of structures. Part 1: General provisions and buildings; Bureau of Indian Standards.

Iyengar R N and Ghosh S 2004 Microzonation of earthquake hazard in Greater Delhi area; *Curr. Sci.* **87** 1193–1202.

Jaiswal K and Sinha R 2007 Probabilistic seismic-hazard estimation for peninsular India; *Bull. Seismol. Soc. Am.* **97** 318–330, https://doi.org/10.1785/0120050127.

Jaiswal K and Sinha R 2006 Probabilistic modeling of earthquake hazard in stable continental shield of the Indian Peninsula; *ISET J. Earthq. Technol.* **43** 49–64.

Joshi G C and Sharma M L 2008 Uncertainties in the estimation of M_{max}; *J. Earth Syst. Sci.* **117** 671–682, https://doi.org/10.1007/s12040-008-0063-5.

Keshri C K, Mohanty W K and Ranjan P 2020 Probabilistic seismic hazard assessment for some parts of the Indo-Gangetic plains, India; *Nat. Hazards* **103** 815–843, https://doi.org/10.1007/s11069-020-04014-8.

Khan M M and Kumar G K 2018 Statistical completeness analysis of seismic data; *J. Geol. Soc. India* **91** 749–753, https://doi.org/10.1007/s12594-018-0934-6.

Khan M M, Munaga T, Kiran D N and Kumar G K 2020 Seismic hazard curves for Warangal city in Peninsular India; *Asian J. Civ. Eng.* **21** 543–554, https://doi.org/10.1007/S42107-019-00210-5.

Kramer S L 1996 Geotechnical earthquake engineering; In: *Prentice-Hall International Series in Civil Engineering and Engineering Mechanics*, Prentice-Hall, New Jersey.

Kulkarni R B, Youngs R R and Coppersmith K J 1984 Assessment of confidence intervals for results of seismic hazard analysis; *8th World Conf. Earthq. Eng.*, pp. 263–270.

Lizundia B, Davidson R A, Hashash Y M and Olshansky R 2017 Overview of the 2015 Gorkha, Nepal, earthquake and the earthquake spectra special issue; *Earthq. Spectra* **33(1_suppl)** 1–20, https://doi.org/10.1193/120817EQS252M.

Mandal P, Rastogi B K and Gupta H K 2000 Recent Indian earthquakes; *Seismology* **79** 1334–1346.

McGuire R K and Arabasz W J 1985 An introduction to probabilistic seismic hazard analysis; In: *Geotechnical an Environmental Geophysics: Volume I: Review and Tutorial*, pp. 333–354.

Menon A, Ornthammarath T, Corigliano M and Lai C G 2010 Probabilistic seismic hazard macrozonation of Tamil Nadu in Southern India; *Bull. Seismol. Soc. Am.* **100** 1320–1341, https://doi.org/10.1785/0120090071.

Mohanty W K, Mohapatra A K and Verma A K 2015 A probabilistic approach toward earthquake hazard assessment using two first-order Markov models in Northeastern India; *Nat. Hazards* **75** 2399–2419, https://doi.org/10.1007/s11069-014-1438-3.

Mohanty W K and Verma A K 2013 Probabilistic seismic hazard analysis for Kakrapar atomic power station, Gujarat, India; *Nat. Hazards* **69** 919–952, https://doi.org/10.1007/s11069-013-0744-5.

Mohindra R, Nair A K, Gupta S, Sur U and Sokolov V 2012 Probabilistic seismic hazard analysis for Yemen; *Int. J. Geophys.* 1–14, https://doi.org/10.1155/2012/304235.

Musson R M 2000 The use of Monte Carlo simulations for seismic hazard assessment in the UK; *Ann. Geofis* **43** 1–9.

Nath S K and Thingbaijam K K 2012 Probabilistic seismic hazard assessment of India; *Seismol. Res. Lett.* **83** 135–149, https://doi.org/10.1785/gssrl.83.1.135.

NDMA 2010 Development of probabilistic seismic hazard map of India; Technical report by national disaster management authority, Government of India.

Ordaz M and Arroyo D 2016 On uncertainties in probabilistic seismic hazard analysis; *Earthq. Spectra* **32** 1405–1418, https://doi.org/10.1193/052015EQS075M.

Ornthammarath T, Lai C G, Menon A, Corigliano M, Dodagoudar G R and Gonavaram K 2008 Seismic hazard at the historical site of Kancheepuram in Southern India; *14th World Conf. Earthq. Eng.*, pp. 1–8.

Pailoplee S, Sugiyama Y and Charusiri P 2009 Deterministic and probabilistic seismic hazard analyses in Thailand and adjacent areas using active fault data; *Earth Planet. Sp.* **61** 1313–1325, https://doi.org/10.1186/BF03352984.

Panza G F, Irikura K, Kouteva-Guentcheva M, Peresan A, Wang Z and Saragoni R 2011 Advanced seismic hazard assessment; *Pure Appl. Geophys.* **168** 1–9, https://doi.org/10.1007/s00024-010-0179-9.

Patil S G, Menon A and Dodagoudar G R 2018 Probabilistic seismic hazard at the archaeological site of Gol Gumbaz in Vijayapura, South India; *J. Earth Syst. Sci.* **127** 1–24, https://doi.org/10.1007/s12040-018-0917-4.

Peláez Montilla J A, López Casado C and Henares Romero J 2002 Deaggregation in magnitude, distance, and azimuth in the south and west of the Iberian Peninsula; *Bull. Seismol. Soc. Am.* **92** 2177–2185, https://doi.org/10.1785/0120010295.

Raghu Kanth S T G and Iyengar R N 2006 Seismic hazard estimation for Mumbai city; *Curr. Sci.* **91** 1486–1494.

Raghu Kanth S T G and Iyengar R N 2007 Estimation of seismic spectral acceleration in Peninsular India; *J. Earth Syst. Sci.* **116** 199–214, https://doi.org/10.1007/s12040-007-0020-8.

Rajendran K and Rajendran C P 2003 Seismogenesis in the stable continental regions and implications for hazard assessment: Two recent examples from India; *Curr. Sci.* **85** 896–903.

Ramkrishnan R, Kolathayar S and Sitharam T G 2019 Seismic hazard assessment and land use analysis of Mangalore city, Karnataka, India; *J. Earthq. Eng.* **25(12)** 2349–2270, https://doi.org/10.1080/13632469.2019.1608333.

Roshan A D and Basu P C 2010 Application of PSHA in low seismic region: A case study on NPP site in peninsular India; *Nucl. Eng. Des.* **240(10)** 3443–3454, https://doi.org/10.1016/j.nucengdes.2010.04.037.

Sabetta F, Lucantoni A, Bungum H and Bommer J J 2005 Sensitivity of PSHA results to ground motion prediction relations and logic-tree weights; *Soil Dyn. Earthq. Eng.* **25** 317–329, https://doi.org/10.1016/j.soildyn.2005.02.002.

Scordilis E M 2006 Empirical global relations converting M_S and m_b to moment magnitude; *J. Seismol.* **10** 225–236, https://doi.org/10.1007/S10950-006-9012-4.

SEISAT 2000 *Seismotectonic Atlas of India and its Environs*; Published by Geological Survey of India.

Shukla J and Choudhury D 2012 Estimation of seismic ground motions using deterministic approach for major cities of Gujarat; *Nat. Hazards Earth Syst. Sci.* **12** 2019–2037, https://doi.org/10.5194/NHESS-12-2019-2012.

Singh N N, Deviprasad B S, Krishna P H and Kumar G K 2015 Probabilistic seismic hazard analysis for Warangal considering single seismogenic zoning; In: *50th Indian Geotechnical Conference*.

Sitharam T G and Kolathayar S 2018 Earthquake hazard assessment: India and adjacent areas; CRC Press.

Sitharam T G, James N, Vipin K S and Raj K G 2012 A study on seismicity and seismic hazard for Karnataka State; *J. Earth Syst. Sci.* **121** 475–490, https://doi.org/10.1007/s12040-012-0171-0.

Sitharam T G, Kolathayar S and James N 2015 Probabilistic assessment of surface level seismic hazard in India using topographic gradient as a proxy for site condition; *Geosci. Front.* **6** 847–859, https://doi.org/10.1016/j.gsf.2014.06.002.

Smriti Mallapaty 2022 Deadly Afghanistan; *Nature* **607** 433.

Sreejaya K P, Raghu Kanth S T G, Gupta I D, Murty C V and Srinagesh D 2022 Seismic hazard map of India and neighbouring regions; *Soil Dyn. Earthq. Eng.* **163** 107505, https://doi.org/10.1016/j.soildyn.2022.107505.

Stepp J C 1974 Analysis of completeness of the earthquake sample in the puget sound area and its effect on statistical estimates of earthquake hazard; In: *1st International conference microzonation Seattle*.

Sulastri S, Sunardi B, Gunawan M T and Gunawan T 2021 Application of the hybrid GMPE for seismic hazard analysis at Banjar City, West Java; *Inter. J. Dyn. Eng. Sci. (IJDES)* **6(2)** 67–73.

Surve G, Kanaujia J and Sharma N 2021 Probabilistic seismic hazard assessment studies for Mumbai region; *Nat. Hazards* **107** 575–600, https://doi.org/10.1007/s11069-021-04596-x.

Thaker T P, Rathod G W, Rao K S and Gupta K K 2012 Use of seismotectonic information for the seismic hazard analysis for Surat city, Gujarat, India: Deterministic and probabilistic approach; *Pure Appl. Geophys.* **169** 37–54, https://doi.org/10.1007/s00024-011-0317-z.

Tinti S and Mulargia F 1985 Effects of magnitude uncertainties on estimating the parameters in the Gutenberg-Richter frequency-magnitude law; *Bull. Seismol. Soc. Am.* **75** 1681–1697, https://doi.org/10.1785/BSSA0750061681.

Tsapanos T M 1990 *b*-Values of two tectonic parts in the circum-pacific belt; *Pure Appl. Geophys.* **134** 229–242, https://doi.org/10.1007/BF00876999.

Uhrhammer R A 1991 Northern California seismicity; *Neotectonics North Am.* 99–106, https://doi.org/10.1130/DNAG-CSMS-NEO.99.

Vigny C, Simons W J, Abu S, Bamphenyu R, Satirapod C, Choosakul N, Subarya C, Socquet A, Omar K, Abidin H Z and Ambrosius B A 2005 Insight into the 2004 Sumatra-Andaman earthquake from GPS measurements in southeast Asia; *Nature* **436(7048)** 201–206, https://doi.org/10.1038/nature03937.

Vipin K S, Anbazhagan P and Sitharam T G 2009 Estimation of peak ground acceleration and spectral acceleration for South India with local site effects: Probabilistic approach; *Nat. Hazards Earth Syst. Sci.* **9** 865–878, https://doi.org/10.5194/NHESS-9-865-2009.

Vipin K S and Sitharam T G 2013 Delineation of seismic source zones based on seismicity parameters and probabilistic evaluation of seismic hazard using logic tree approach; *J. Earth Syst. Sci.* **122** 661–676, https://doi.org/10.1007/s12040-013-0300-4.

Walter T R, Wang R, Luehr B G, Wassermann J, Behr Y, Parolai S, Anggraini A, Günther E, Sobiesiak M, Grosser H and Wetzel H U 2008 The 26 May 2006 magnitude 6.4 Yogyakarta earthquake south of Mt. Merapi volcano: Did lahar deposits amplify ground shaking and thus lead to the

disaster?; *Geochem. Geophys. Geosyst.* **9(5)**, https://doi.org/10.1029/2007GC001810.

Wiemer S 2001 A software package to analyze seismicity: ZMAP; *Seismol. Res. Lett.* **72** 373–382, https://doi.org/10.1785/GSSRL.72.3.373.

Wiemer S, Giardini D, Fäh D, Deichmann N and Sellami S 2009 Probabilistic seismic hazard assessment of Switzerland: Best estimates and uncertainties; *J. Seismol.* **13** 449–478, https://doi.org/10.1007/s10950-008-9138-7.

Williams J N, Werner M J, Goda K, Wedmore L N, De Risi R, Biggs J, Mdala H, Dulanya Z, Fagereng Å, Mphepo F and Chindandali P 2023 Fault-based probabilistic seismic hazard analysis in regions with low strain rates and a thick seismogenic layer: A case study from Malawi; *Geophys. J. Int.* **233** 2172–2206, https://doi.org/10.1093/gji/ggad060.

Corresponding editor: W K Mohanty